1

INTRODUCTION TO AMORPHOUS SOLID DISPERSIONS

George Zografi[1] and Ann Newman[2]

[1]*University of Wisconsin-Madison, Madison, WI, USA*
[2]*Seventh Street Development Group, Lafayette, IN, USA*

1.1 INTRODUCTION

Over the years one of the major goals of synthetic chemists has been to provide the crystalline form of any active pharmaceutical ingredient (API) being introduced into pharmaceutical development. This is primarily because the symmetrical three-dimensional long-range order and the relatively tight packing of molecules in a crystal lattice most often ensure a high level of chemical purity and solid-state stability. At the same time, an API being developed for oral administration in a solid dosage form generally requires sufficient aqueous solubility upon contact with *in vitro* and *in vivo* dissolution media in order to obtain optimal rates of dissolution and acceptable oral bioavailability. The importance of aqueous solubility in affecting dissolution rates can be shown with the classical Noyes–Whitney equation [1]:

$$\mathrm{d}C/\mathrm{d}t = k_D A(C_s - C_t), \tag{1.1}$$

where $\mathrm{d}C/\mathrm{d}t$ is the dissolution rate, k_D is the dissolution rate constant (dependent on the stirring rate and the diffusion constant), A is the total surface area of the drug particles, C_s

Pharmaceutical Amorphous Solid Dispersions, First Edition. Edited by Ann Newman.

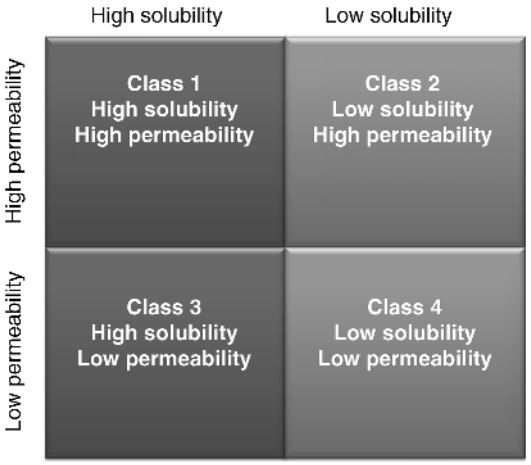

Figure 1.1. Biopharmaceutical classification systems (adapted from Ref. 2).

is the aqueous saturation solubility of the drug, and C_t is the concentration dissolved at time t. Based on this equation, it can be seen that all other factors being constant, the rate of dissolution is proportional to the surface area of the solute particle and to the solubility of the drug. Consequently, drugs with low aqueous solubility would be expected to exhibit low dissolution rates and, likely, poor oral bioavailability. The importance of the rate of dissolution and hence aqueous solubility in acting as a determinant of oral absorption was formally recognized with the establishment of the Biopharmaceutics Classification System (BCS) [2], where, as illustrated in Figure 1.1, the API is classified into four categories: classes 1 and 3 containing molecules with high aqueous solubility, and classes 2 and 4 containing molecules with low solubility; molecules in classes 3 and 4 also exhibit poor biological membrane permeability, another deterrent to drug absorption. Interestingly, over the past few decades there has been a significant increase in the number of APIs under development that have fallen into BSC classes 2 and 4 because of solubility problems. This decrease in dissolution of crystalline API appears to correlate with a corresponding increase in the number of API molecules in the development process that have larger average molecular weights, higher melting temperatures, and a higher degree of hydrophobicity than that observed in previous years. As a consequence, during the past few years, there has been a significantly increased effort to develop strategies that might serve to enhance the rate of dissolution of an API by means of formulation, chemical modification, or processing.

Based on Equation 1.1, we can conclude that there are two major factors that can be used as a basis for enhancing dissolution rates of poorly water-soluble crystalline APIs sufficiently to have some controllable influence on increasing oral bioavailability. These are the surface area of the solid exposed to the aqueous medium and the solubility of the solid in aqueous media. Strategies for enhancing dissolution can be divided further into (i) formulation and processing, (ii) chemical modification, and (iii) use of "high-energy" structurally disordered physical forms of the solid. Starting with the crystalline API, the formulator can simply reduce the particle size of crystalline materials to increase their

specific surface area (area per unit mass). Very significant increases in dissolution rate, for example, have been attained by producing particles with diameters on the order of 100–300 nm. One also can increase dissolution rates by adding solubilizers to the formulation, such as surfactants, or complexing agents, such as cyclodextrins, which help to produce a supersaturated solution when the API encounters an aqueous medium. Surfactants can also act as wetting agents to improve access of the aqueous medium to hydrophobic API, thus effectively increasing the available surface area. High levels of supersaturation, upon contact with water, can also be obtained by dissolving the API in liquid lipid-based formulations and administering the product in hard or soft capsule form. Such an approach tends to produce a supersaturated solution upon exposure to aqueous dissolution media. Alteration of the API chemically by forming more highly water-soluble crystalline salts or cocrystals, when possible, can be a very efficient way of increasing dissolution rates as long as the dissolved form of the API can be maintained in a supersaturated state relative to that of the crystalline "free form" of the API itself. Finally, since the high lattice energy of an API crystal, as often reflected at high melting temperatures, can serve as an impediment to attaining adequate thermodynamic solubility, any approach that can change, reduce, or eliminate the crystal lattice energy should be able to enhance the apparent solubility. For example, liquid forms of molecules will generally exhibit greater solubility than their crystalline counterparts (supersaturation), all other factors being equal. Indeed, it is well known that higher energy "less-stable" polymorphic crystal forms of an API generally exhibit greater solubility than the most stable form. It has also been shown that disorder in the crystal lattice introduced as crystal defects can serve to increase dissolution from the defect sites relative to that from the less defective crystal. Consequently, it is not surprising that complete elimination of long-range three-dimensional order in the crystal by forming the amorphous form of an API can greatly enhance apparent solubility and rates of dissolution. Of course, since the amorphous state represents a high-energy form relative to the crystal, this approach can be useful only as long as a supersaturated solution of API can be maintained in the aqueous medium over the time period required for gastrointestinal absorption. Since the overall theme of this book deals with amorphous API-polymer solid dispersions designed to provide enhanced oral bioavailability by creating such supersaturation, it will be useful in this introductory chapter to review some of the important physicochemical characteristics of amorphous solids as single components and as mixtures of API with other formulation components that might be used to enhance oral bioavailability in drug products. A brief discussion of API-polymer amorphous dispersions, in particular, will serve as an introductory overview of various principles that will be applied in more detail throughout the rest of the book.

1.2 FORMATION OF THE AMORPHOUS STATE AND THE GLASS TRANSITION TEMPERATURE

Let us first consider a single-component system such as an API in its most stable crystalline form. From a classical free energy–temperature diagram [3], as illustrated in Figure 1.2, we can observe a significant reduction in the free energy per mole of the

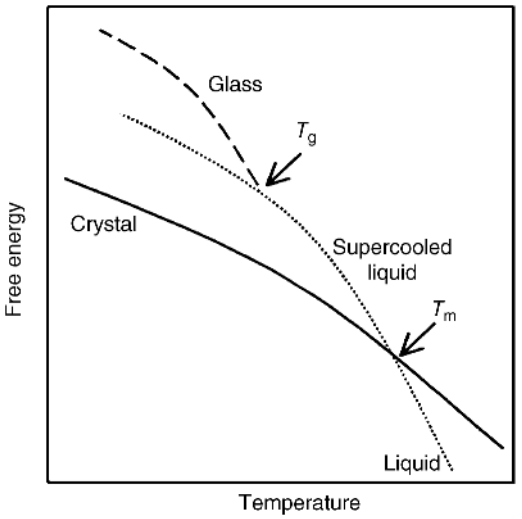

Figure 1.2. Free energy–temperature diagram for a single-component system (reproduced with permission from Ref. 3. Copyright 2001, Elsevier).

crystal as the temperature of the sample is increased until we reach the melting temperature T_m where the crystal undergoes a spontaneous first-order conversion to the liquid form, with the liquid now in a lower free energy state. If the liquid is slowly cooled to below T_m, and there is sufficient time for nucleation and crystal growth to occur, the system will revert to the equilibrium state of the crystal. If, however, as seen in Figure 1.2, the liquid sample is cooled rapidly through T_m so as to kinetically avoid crystallization, the system will show no discontinuities at T_m and maintain the equilibrium properties of the liquid as a supercooled liquid that is metastable relative to the crystal. Upon further cooling and as the viscosity of the supercooled liquid increases and diffusive motions of the molecules decrease, equilibrium can no longer be maintained and a distinct discontinuity in the free energy–temperature diagram occurs with the formation of the unstable glassy state. This occurs at a distinct temperature, designated the glass transition temperature T_g, the value of which for a particular molecule under the same processing conditions is determined by the molecular weight, degree of polarity, and the effect of molecular shape on the closeness of molecular packing. For example, the more polar the solid or the higher the molecular weight, the greater the value of T_g, while the bulkier the shape of the molecule and poorer the packing, the lower the T_g. The value of T_g is experimentally determined most conveniently by using differential scanning calorimetry, where the heat capacity can be measured as the sample temperature is continuously changed at a constant rate from low temperatures to the melting temperature. Because of structural changes that bring about changes in the rate of molecular motions, the heat capacity generally undergoes a distinctly abrupt change at T_g, as illustrated in Figure 1.3. In general, it has been shown that the viscosity of an organic liquid at T_m is on the order of 10^{-2} Pas, while at T_g this value has increased to about 10^{12} Pas, a 14 order of magnitude change! Since this point of discontinuity is associated with such a significant change in viscosity as cooling occurs, experimental values of T_g will depend to a small extent on the rate of cooling: the faster the rate of

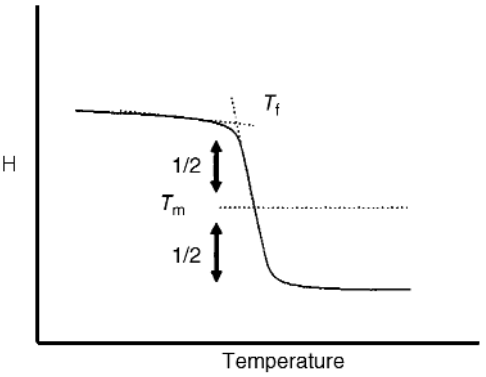

Figure 1.3. Heat capacity change at the glass transition indicating the onset glass transition temperature T_{gonset} and the midpoint glass transition temperature T_{gmid}.

cooling, the greater the T_g. Thus, in reporting the T_g for a particular material, it is important to indicate the conditions used to measure T_g and to form the glassy state. However, despite small differences in T_g that arise with different methods of preparation, it has been observed for small organic molecules and organic polymers exhibiting a crystalline state that when temperature is expressed in Kelvin, the T_g can be approximated empirically to be equal to a value of about $0.67T_m$ [4,5]. Such an empirical equation can be very helpful in determining the likely region of temperature where the T_g of a newly formed amorphous API may be located. Since molecules are kinetically "trapped" in the glassy state, it is not surprising that different rates of cooling generally lead to glasses with slightly different structural features. Because of this, and because the glass is unstable relative to the supercooled liquid, when held at temperatures close to, but below, T_g, the solid generally will exhibit an ability to slowly "age" or "anneal" with accompanying thermodynamic changes, such as a loss of free energy, enthalpy, and entropy and an increase in density, closer to values expected for the supercooled liquid, as illustrated in Figure 1.4 [6]. Thus, we can conclude that determining T_g is central to any characterization of amorphous solids, and that the method

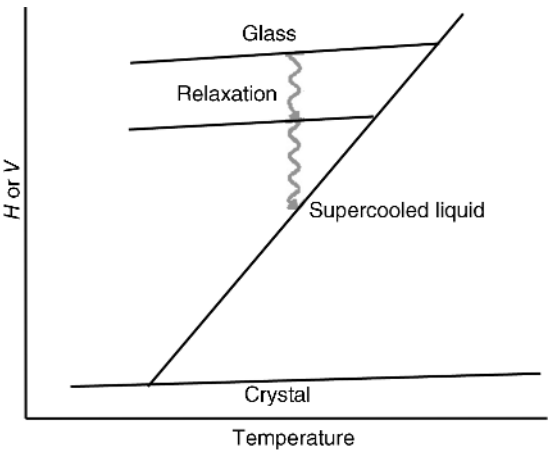

Figure 1.4. Relaxation of a glass toward the equilibrium liquid state due to physical aging.

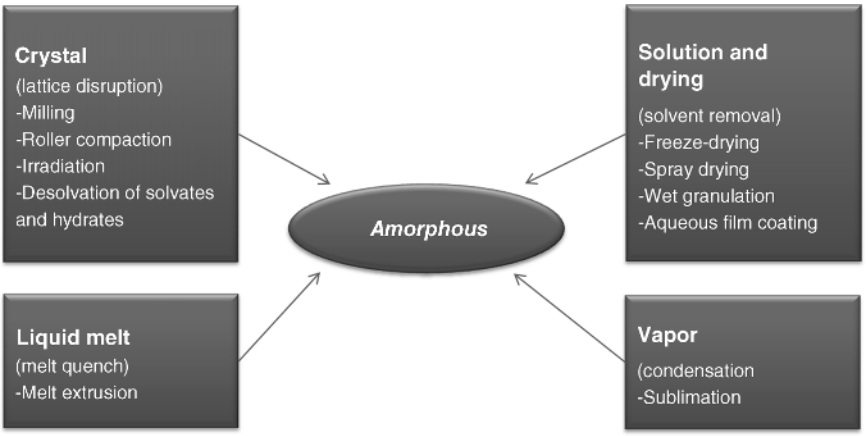

Figure 1.5. Various methods of producing the amorphous state.

of preparation of amorphous solids must be outlined in detail when reporting any value of T_g.

In this regard, so far we have focused only on the preparation of an amorphous solid by melting the crystalline form and then rapidly supercooling the melt to well below the melting temperature so as to avoid crystallization. Indeed, this is the basis for using the hot melt extrusion method to produce amorphous solid dispersions (ASDs), a topic that will be discussed more fully in later chapters. However, as described in Figure 1.5, it is also possible to produce amorphous forms by rapidly condensing molecules directly from the vapor state at low temperatures, or by causing molecules to rapidly precipitate from solution, where in both cases crystallization is kinetically avoided. Although preparation from the vapor state is not currently used as a process to form amorphous pharmaceutical products, there is evidence that such a method can lead to unusually stable glasses [7]. Precipitation from solution to form an amorphous solid is the basis for the widely used processes of lyophilization and spray drying (SD), where lyophilization has proved particularly useful in forming sterile amorphous protein products for parenteral use, and spray drying for the development of solid dispersions for oral and pulmonary use. As seen in Figure 1.5, it is also possible to form the amorphous state directly from a crystal by introducing mechanical stress that is sufficient to create crystal defects that eventually coalesce into a completely amorphous form [8]. Likewise, it has been shown that amorphous forms can be created by the dehydration of crystal hydrates [9] or by the desolvation of crystal solvates [10], where in both cases the desolvated crystal lattice collapses because of the free volume left by removing the solvent from the crystal lattice. Although such methods that disrupt the crystal lattice have not yet been found practical for the preparation of pharmaceutical amorphous systems on a large scale, the importance of such phenomena has been demonstrated in situations where crystalline solids are inadvertently rendered partially amorphous by processes such as milling and drying, leading to small amounts of disorder and unanticipated

solid-state instabilities [11]. In conclusion, given that different methods used to form amorphous solids can lead to glasses with somewhat different properties, it is important to recognize that the various pharmaceutical processes used to produce robust amorphous drug products of high quality and performance must be under very careful control with regard to time, temperature, and other process conditions.

1.3 STRUCTURE OF AMORPHOUS SOLIDS

The structural arrangement of molecules in crystals, as determined by intermolecular interactions and molecular size and shape, can be described in terms of a specific local structure reflected by the geometric arrangement of molecules within the unit cell, and the long-range symmetrical three-dimensional extension of the repeating unit cells. The same molecule in the crystalline state may be able to form in different unit cells, and, therefore, to exist in distinctly different polymorphic forms. Single-crystal X-ray diffraction techniques are used to determine the arrangement of molecules in the unit cell, while, as shown in Figure 1.6, powder X- ray diffraction measurements (PXRD) reveal distinct diffraction peaks at characteristic scattering angles that represent the various planes of long-range symmetry within the crystal and can be used to identify the crystal form. Liquids and supercooled liquids, on the other hand, having lost the long-range three-dimensional order of the crystal will exhibit PXRD patterns that are devoid of these distinct peaks, rather than exhibiting a broad halo of X-ray intensity, as seen in Figure 1.6. From extensive studies of liquids and supercooled liquids, it has been

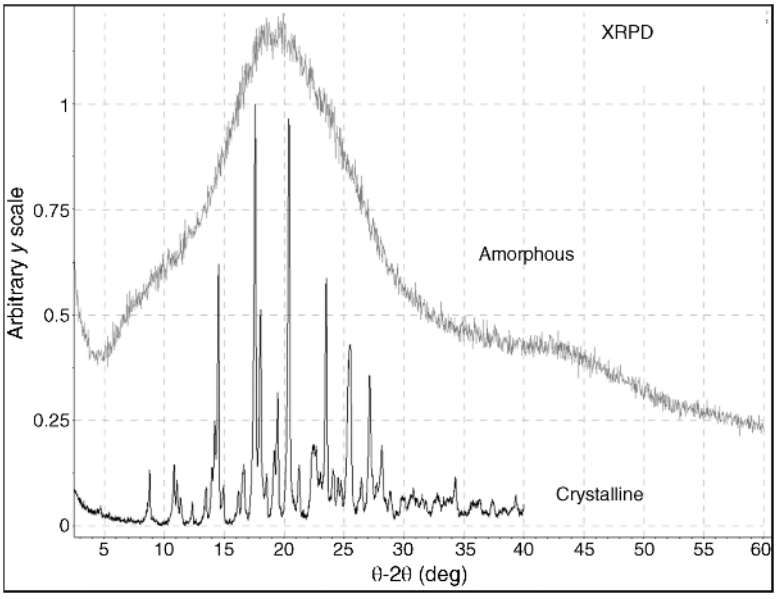

Figure 1.6. Typical powder X-ray diffraction patterns for crystalline and amorphous forms.

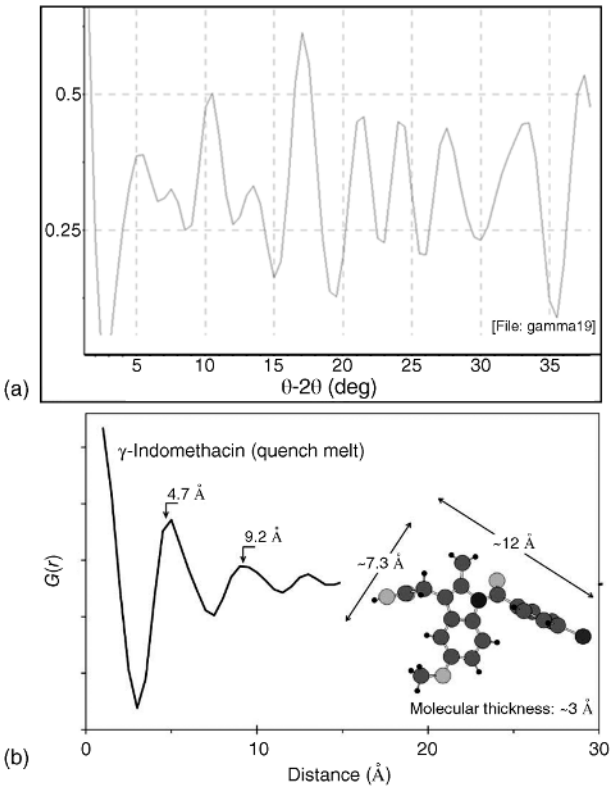

Figure 1.7. Pairwise distribution function. (a) Crystalline indomethacin. (b) Amorphous indomethacin (reproduced with permission from Ref. 12. Copyright 2006, Springer).

established that they maintain a distinct local arrangement of molecules over at least nearest-neighbor (NN) and next nearest-neighbor (NNN) distances, wherein the arrangement is similar to, and sometimes the same as, that in the corresponding crystal unit cell. To more quantitatively describe the local structure of an amorphous solid, it is possible to use PXRD data to determine the pair distribution function (PDF), which is a parameter that describes the probability $G(r)$ of finding the relative location of two atoms within a given volume when they are separated by a radial distance r, as shown in Equation 1.2 [12,13]:

$$G(r) = 4\pi r[\rho(r) - \rho_0], \tag{1.2}$$

where $\rho(r)$ and ρ_0 are the local and average atomic densities, respectively. As shown in Figure 1.7, for the amorphous and crystalline forms of the drug indomethacin, distinct peaks in a plot of $G(r)$ versus distance occur for amorphous indomethacin at distances that correspond very closely to the NN and NNN distances expected for the indomethacin molecule, but not out to greater distances [12]. On the other hand,

similar repeating PDF peaks extend out to much greater distances for the crystal, reflecting the greater long-range order in the crystal. From this and many other studies using estimates of the PDF profile of amorphous solids, it has been possible to conclude that local structures of amorphous solids, closely related to the unit cell of the corresponding crystal, are maintained in the amorphous state under all conditions, despite the lack of long-range order.

Although amorphous solids, like liquids, do not exhibit long-range order, it is of interest to have some understanding of the manner in which molecules are organized beyond NN and NNN distances to form the bulk solid structure. Structural features of amorphous solids in the supercooled state at temperatures above T_g can best be understood by what is generally known about the structure of simple liquids, where it is assumed that molecules are packed randomly as polyhedral clusters that minimize the overall free energy of the system without crystallizing [14]. Typically, the densest possible packing of spheres of the same size, as in a face-centered cubic crystal, would have the spheres occupying a maximum of 0.74 of the total volume occupied by the material, while the remainder would be taken up by the volume fraction of void space equal to 0.26. The random close packing (RCP) model is an empirical statistical model that considers the packing of an object that has almost no period packing structure, as when pouring spheres into a container. Mathematical modeling of such a system reveals that at closest packing the spheres must occupy a volume fraction of <0.64 and that such a model can describe the structure of simple liquids quite well. In general, it appears that molecules in the supercooled liquid state contain fairly homogeneously sized polyhedral structures down to temperatures roughly on the order of $1.5T_g$, at which point the molecular structures then become distorted by "jamming up" into a more spatially heterogeneous system with a distribution of cluster sizes [15]. Such a temperature is generally termed the crossover temperature T_c. As will be discussed more fully subsequently, because of such structural changes, at temperatures between T_g and T_c, the mobility of molecules in the system will undergo decrease by orders of magnitude as the system becomes more "solid-like" and approaches the glassy state. When the system goes below T_g into the glassy state, we would expect there to be further "jamming" and a tendency for the molecules to readjust into a distinctly different structure, while retaining essentially the same local structure. Indeed, application of a modified form of the RCP to organic glasses reveals that its structure is best described by small highly dense local clusters of molecules having a size of roughly 2.0–2.5 nm, surrounded by interfacial regions of less densely packed molecules in a higher state of energy [12]. Such a structure might be considered analogous to a polycrystalline mass, containing many small crystallites surrounded by a higher energy region of grain boundaries. An analysis of amorphous indomethacin in the glassy state, for example, led to a structure consistent with this picture, as illustrated in Figure 1.8 [12]. Further analysis suggested that the higher energy region, termed the microstructure, represents about 10% of the total mass, and that it was very likely the region of the glass that spontaneously anneals or ages when held at temperature just below T_g, as illustrated earlier in Figure 1.4. It is also believed to be the likely region that acts to retard the rate at which the local domains nucleate and undergo crystallization.

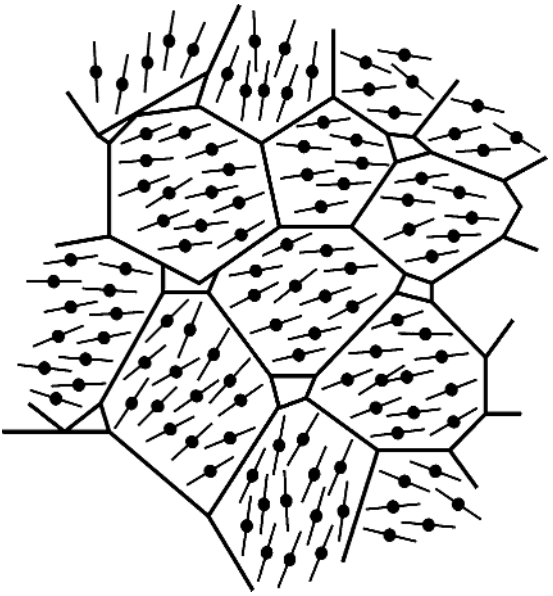

Figure 1.8. Schematic representation of the structure of an amorphous solid in the glassy state (reproduced with permission from Ref. 12. Copyright 2006, Springer).

1.4 MOLECULAR MOBILITY IN AMORPHOUS SOLIDS

As inferred from the discussion so far, during the process of forming amorphous solids, the thermodynamic properties shown in Figure 1.2 are strongly influenced by the kinetic properties of the system, as reflected in the levels of allowed molecular motion, often referred to as molecular mobility. For the present discussion, molecular motions can be placed into three broad categories: (i) high-frequency intramolecular motions, including harmonic bond vibrational and spinning modes; (ii) whole molecule or polymer segmental secondary "caged" or hindered motions, generally referred to as Johari–Goldstein β-relaxations; and (iii) primary whole molecule or polymer segmental translational and rotational diffusive α-relaxations. Central to the properties of molecules in the amorphous state are the highly cooperative diffusive translational and rotational motions that occur at various temperatures above and below T_g. The rate of such translational and rotational motions can be expressed in terms of diffusion constant D_{trans} and D_{rot}, respectively, where for a sphere of radius r in a liquid with viscosity η and at temperature T in the Stokes–Einstein equation,

$$D_{trans} = (k_B T)/(6\pi r\eta), \tag{1.3}$$

and in the Debye equation,

$$D_{rot} = (k_B T)/8\pi r^3\eta), \tag{1.4}$$

where k_B is the Boltzmann constant. From these equations we can see that at constant molecular size, the rate of such diffusive motions will be critically controlled by both temperature and viscosity.

Another more general way to express molecular mobility quantitatively is to define the relaxation time τ, a parameter that directly indicates the timescale over which a single rotation takes place or the time over which a molecule undergoes translation across a given reference distance; the greater the viscosity and hence the smaller the diffusion coefficient, the greater the translational or rotational relaxation time. To determine the value of τ under a given set of conditions, one can experimentally perturb the system out of equilibrium mechanically, electrically, or magnetically and observe the rate $\phi(t)$ at which the property returns toward the equilibrium state. Dynamic mechanical analysis (DMA) is generally used to measure the rate of relaxation and viscosity; however, primary relaxations can also be measured by electrical perturbation of dipoles in the molecule and measurement of the dipole relaxation back toward an equilibrium state using dielectric spectroscopy (DES). For a system exhibiting a single mode of relaxation that follows first-order kinetics, such as a pure liquid above its melting temperature, one can write

$$\phi(t) = \exp[-t/\tau], \tag{1.5}$$

where τ is the reciprocal of the first-order rate constant. In such a case, one would expect the temperature dependence of τ to follow the Arrhenius equation:

$$\tau(T) = \tau_0 \exp[E_a/RT], \tag{1.6}$$

where τ_0 is the relaxation time at the high temperature limit, on the order of 10^{-12} s, and E_a is the activational energy associated with the process. Indeed, equilibrium liquids generally exhibit Arrhenius kinetics. Supercooled liquids at temperatures approaching T_g, however, appear to exhibit more than a single relaxation time generally described by a "stretch" exponential form of Equation 1.5 that takes into account this distribution of relaxation modes. For example, a widely applicable empirical equation in such situations is the Kohlrausch–Williams–Watts (KWW) equation:

$$\phi(t) = \exp[-t/\tau]^{\beta}, \tag{1.7}$$

where τ is the average relaxation time and β represents the distribution of different relaxation times, with values falling between 0 and 1; a value of 1 indicates a single mode of relaxation and smaller values represent an increasing number of relaxation modes. Most amorphous systems of pharmaceutical interest yield values of β in the range of 0.3–0.6 [16]. When such an equation is applicable, the temperature dependence of τ can be expressed by the nonexponential empirical Vogel–Tammen–Fulcher (VTF) equation:

$$\tau(T) = \tau_0 \exp[DT_0/(T - T_0)], \tag{1.8}$$

where D and T_0 are constants. D is called the "strength parameter," an indication of the activation energy of the diffusive relaxation process, and T_0 is the temperature at which

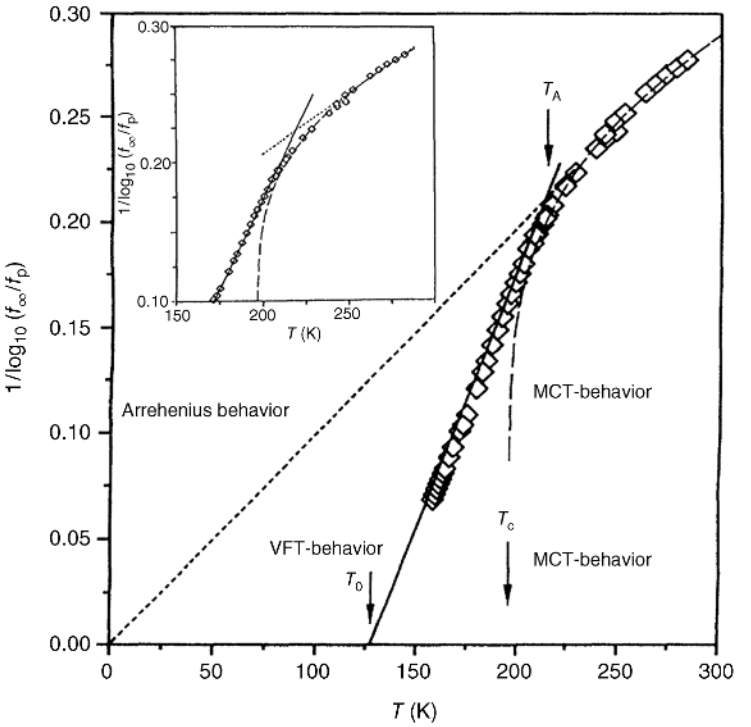

Figure 1.9. A plot representing the reciprocal of relaxation time versus temperature for propylene carbonate (reproduced with permission from Ref. 17. Copyright 1993, American Physical Society).

$\tau(T)$ eventually would reach infinity or zero molecular mobility. For small organic molecules, T_0 generally falls between 40 and 70 K below T_g. Figure 1.9 provides an example of a plot of $1/\tau$ versus T for amorphous propylene carbonate, in the supercooled equilibrium state, having a T_g of 150 K; decreases in the parameter represented on the y-axis reflect an increase in relaxation time or increase in viscosity [17]. Here, we can see that at temperatures above 225 K, or $\sim 1.5T_g$, relaxation times appear to follow Arrhenius kinetics (Equation 1.6) as expected for an equilibrium liquid with a single mode of relaxation. At a temperature labeled T_A, equal to the "crossover temperature" T_c, previously discussed, however, we can observe in Figure 1.9 that there is a marked discontinuity, where the increase in relaxation time now follows the VTF equation (Equation 1.8) with much higher values of relaxation time than predicted by Equation 1.6. Note also in Figure 1.9 the extrapolation of relaxation times to a value of T_0, as presented in Equation 1.8. The data presented in Figure 1.9 show that at temperatures above T_A (T_c), the supercooled liquid is structurally similar to the equilibrium liquid. However, as the system is cooled to below T_c, but above T_g, the supercooled liquid appears to exhibit structural changes and spatial heterogeneity that give rise to multiple modes of relaxation and a very rapid increase in the average τ as the temperature approaches T_g [15]. An

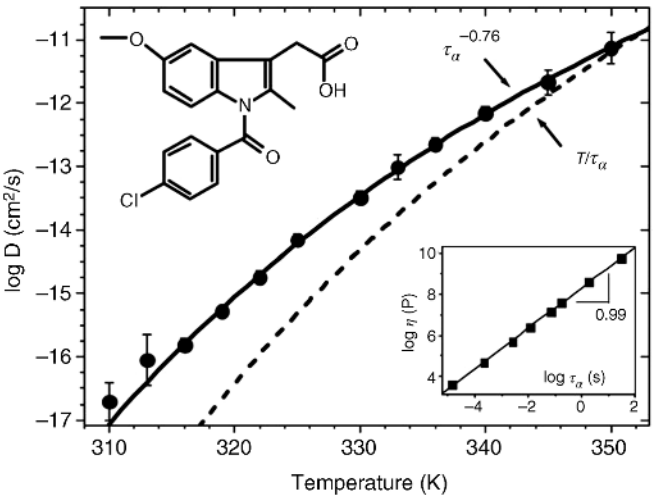

Figure 1.10. Diffusion Coefficients and Rate of Crystal Growth vs. Temperature for Indomethacin Above Its Glass Transition Temperature (experimental points); Expected Diffusion coefficients From Measured Values of Viscosity Assuming the Application of the Stokes-Einstein Equation (see Equation 1.3 in text) (Reproduced with permission from Ref. 18. Copyright © 2011 Royal Society of Chemistry).

indication of the significant structural changes taking place at T_c is provided by the observation, shown in Fig 1.10, that at temperatures below T_c, the relationship between the translational diffusion coefficient and viscosity, as expressed in Equation 1.3, the Stokes–Einstein equation, no longer follows as the temperature dependence of viscosity is uncoupled from that for the diffusion coefficient [18].

From the previous discussion it is clear that the rate at which viscosity and hence diffusive relaxation times increase as the supercooled liquid is cooled toward T_g is an indication of the structural changes caused by changes in molecular packing and intermolecular interactions. Consequently, we would expect such changes to be related to the chemical structure and molecular size and shape of the material and to reflect the activational energy associated with such changes. To put this on a quantitative basis, Angell [19] coined the term fragility and defined it in terms of a fragility index m:

$$m = d\log\tau/d(T_g/T)^{T=T_g}, \tag{1.9}$$

where m is the initial slope of a plot of log τ versus T_g/T taken at the limit of $T = T_g$; the greater the value of m, the greater the fragility, and hence the greater the change in molecular mobility with temperature. Using T_g/T instead of $1/T$ normalizes the data with respect to the value of T_g and allows direct comparison of materials with different values of T_g. For example, as shown in Figure 1.11, plots of log τ versus T_g/T reveal very different initial slopes for three materials with very different structures: silicon dioxide,

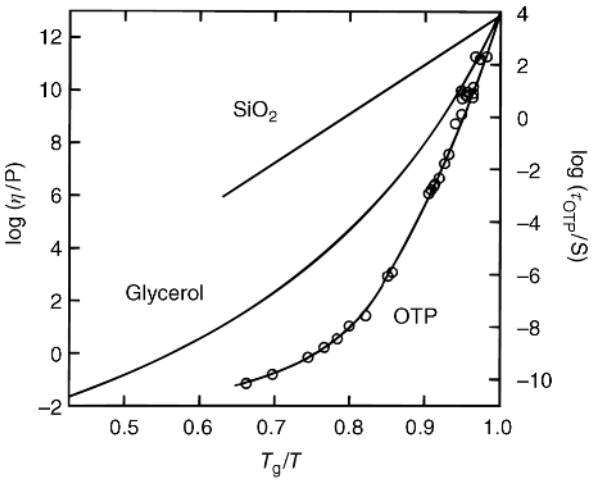

Figure 1.11. Angell Plot for Three Amorphous Materials (Reproduced with permission from Ref. 19. Copyright ©1996 American Chemical Society).

SiO_2, a highly polar inorganic polymeric dense material with $T_g = 1600$ K; *o*-terphenyl, a small molecular weight organic nonpolar molecule with $T_g = 246$ K; and glycerol, a very small molecular weight polar compound with a $T_g = 193$ K. As can be seen, SiO_2 exhibits the smallest value of *m*, *o*-terphenyl the greatest, and glycerol the intermediate behavior. Generally speaking, organic molecules tend to be fairly fragile and most susceptible to structural changes with changing temperature in the vicinity of T_g, while highly polar inorganic polymers, like SiO_2, tend to be more resistant to structural change; materials exhibiting low fragility are generally said to be "strong" supercooled liquids. By combining Equations 1.8 and 1.9, one can express the fragility index in terms of *D*, T_g, and T_0:

$$m = \{D(T_0/T_g)\}/\{[1 - (T/T_0/T_g)]^2 \ln(10)\}, \tag{1.10}$$

where strong liquids exhibit values of *D* in the range of 30 or greater, and fragile liquids have values in the range of 7–15. Indeed, it has been shown that a large group of API molecules have values of *D* that fall in this latter range and thus we can assume that most amorphous API molecules exist as fragile systems with significant sensitivity to changes in temperature above T_g and below T_c [20], the point at which upon cooling molecules tend to "jam" into a spatially heterogeneous state. From previous discussions we have learned that amorphous solids at temperatures lower than T_g form the unstable glassy state that has something like the heterogeneous structure illustrated in Figure 1.8. We also learned that at T_g, the diffusive α-relaxation times on average are on the order of 10^2 s (viscosity of about 10^{12} Pas), indicating that there is still a significant degree of molecular mobility at the initiation of the glassy state. From Equation 1.8 (VTF) we would expect that at temperatures below the crossover temperature T_c, in the supercooled liquid, relaxation times will decrease significantly, the extent of which depends on the level of

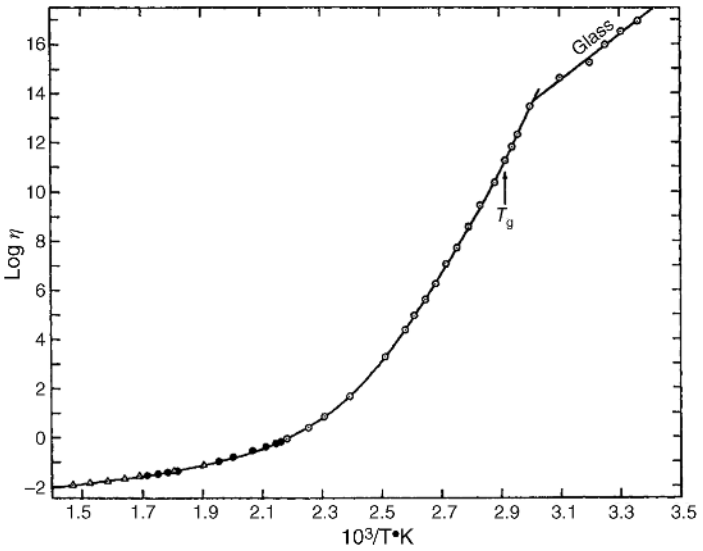

Figure 1.12. Viscosity of amorphous tris-α-naphthylbenzene as a function of the reciprocal of temperature (reproduced with permission from Ref. 21. Copyright 1968, AIP Publishing LLC).

fragility. Since extension of the VTF equation to temperatures below T_g assumes that the supercooled liquid state continues down to T_0, one might expect that the VTF equation would not be able to predict molecular mobility much below T_g. That this is so can be observed in Figure 1.12 where a plot of log η versus $1/T$ for amorphous tris-α-naphthylbenzene indicates that although a discontinuity does not occur at T_g, there is a distinct discontinuity at a temperature that is roughly 15 K below T_g [21]. Below this temperature, viscosity dependence on temperature appears to follow Arrhenius kinetics and exhibit values that are significantly lower than those predicted from the VTF equation. Apparently, closer to T_g there is very rapid aging of the glass toward the supercooled liquid over the time period required to carry out the viscosity measurements (see Figure 1.4 and the earlier discussion of aging of glasses) and viscosity values are those expected for the supercooled liquid. The lower than expected viscosity in the glass would be consistent with the general structure of glasses, as illustrated in Figure 1.8, that contains a microstructure region in which molecules should have higher energy, less density, and higher molecular mobility. Such behavior, that is, greater molecular mobility than predicted from the VTF equation, has also been reported with measurements of relaxation time for amorphous indomethacin at temperatures below T_g using DMA, DES, and thermal analysis [22]. It has been shown further that the extrapolation of relaxation times obtained in the glassy state of indomethacin leads to a value of 3 years (10^8 s) at $T_g - T$ equal to 40 K, 3 years being the desired time of storage generally required for establishing expiration dates of many solid drug products. Thus, long-term stability in this case would require a storage temperature that is about 40 K below T_g. (there will be more discussion of stability subsequently).

An additional factor to consider in discussing molecular mobility in amorphous solids is the fact that molecules at a surface, that is, the solid–vapor interface, which exist at a higher energy than those molecules in the bulk, generally can exhibit greater diffusive molecular motion by means of surface diffusion; the greater degrees of freedom exhibited by a molecule at a surface allows greater lateral translational and rotational motions. This generally is not considered a critical factor with amorphous solids when bulk properties are dominant. However, surface molecular mobility has been shown to be of importance when surface-to-bulk volume ratios become quite great as with thin polymer films or nanosized particles. Indeed, it has been possible to measure bulk and surface diffusion for amorphous indomethacin as a function of temperature, and show that surface diffusion is orders of magnitude greater than bulk diffusion at temperatures well below T_g [23].

1.4.1 Secondary Johari–Goldstein β-Relaxation

So far we have discussed the molecular mobility of amorphous solids in terms of cooperative diffusive translational and rotational motions, generally referred to as primary α-relaxations. Clearly, it is these motions, directly related to viscosity, that determine many of the properties that can affect the pharmaceutical functions and instabilities of amorphous solids. These are also the motions that are responsible for the appearance of the discontinuity in properties that occurs at the glass transition temperature. As already mentioned, molecules in the solid state exhibit other types of motions that occur over very short timescales relative to diffusion. These include intramolecular harmonic bond vibrations and rotations and single molecule or polymer noncooperative segmental hindered or "caged" motions, referred to as Johari–Goldstein (JG) secondary β-motions [24]. Such high-frequency motions, on pico- and nanosecond timescales, are best detected by DES, solid-state nuclear magnetic resonance (SSNMR) spectroscopy, and neutron scattering. The intramolecular harmonic motions do not appear to play an important role in the dynamics of amorphous solids, but the β-motions appear to be important as precursors to events that lead to diffusional motion. Although often difficult to observe in the presence of α-relaxation profiles in DMA or DES measurements, it appears that most organic small molecules undergo JG β-relaxations and that such relaxations involve hindered noncooperative rotational motions of single molecules within the amorphous structure, often envisioned as "molecules rattling in a cage," and located in "islands of mobility" where greater free volume is available. Combined studies using DES and SSNMR indicate that the JG motions occur throughout the amorphous solid, but that roughly 80–90% of the molecules appear to have low amplitudes that are relatively independent of temperature, while 10–20% of the molecules have higher amplitudes and significant temperature dependence [25]. Furthermore, the amplitudes of such motions in the glassy state appear to decrease when the glass undergoes physical aging to more dense structures, as described earlier in Figure 1.4. This suggests that the "islands of mobility" associated with these motions occur primarily in the microstructure region of the glass. The importance of the JG β-motions seems to be related to the fact that these secondary motions provide sufficient critical free volume within the amorphous structure to allow the initiation of the cooperative α-motions that impact many physical properties of the amorphous state [26]. As seen in Figure 1.13, plots of log τ

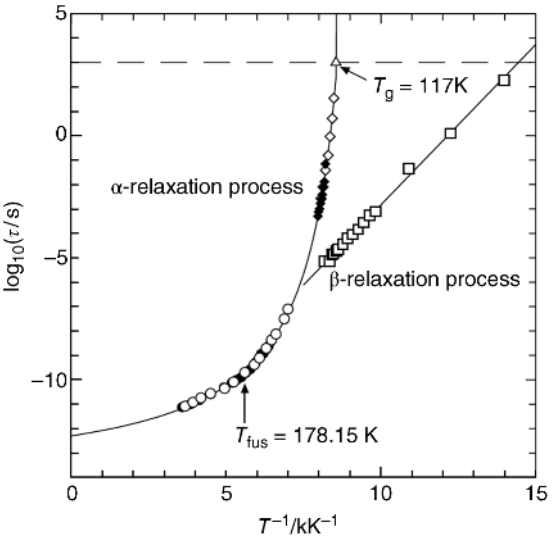

Figure 1.13. Log of α- and β-relaxation times versus reciprocal of temperature for amorphous *ortho*-terphenyl (reproduced with permission from Ref. 27. Copyright 2002, Elsevier).

versus $1/T$ for *o*-terphenyl measurements of α- and β-relaxation times indicate that the two processes decouple at the crossover temperature T_c, discussed previously, and that the β-motions exhibit lower relaxation times than those of α-motions [27]. A term $T_{g\beta}$, obtained by extrapolating values of τ_β to a temperature where these secondary motions cease to be measurable, has been shown to occur at temperatures on the order of 100 K below T_g. This then might be considered the temperature to which a glass should be cooled to eliminate any effects of the JG β-relaxations on the properties of the glass.

1.5 SOLID-STATE CRYSTALLIZATION FROM THE AMORPHOUS STATE

From a thermodynamic perspective, as illustrated in Figure 1.2, molecules in the amorphous state are in a higher free energy state than those in the corresponding crystal at all temperatures. Therefore, we would expect that over some time period the molecules eventually would spontaneously crystallize unless the addition of a crystallization inhibitor and/or a lowering of molecular mobility could act to reduce the rate of crystallization. Such a tendency to crystallize, of course, would negate the use of amorphous forms of API in pharmaceutical products for enhancing aqueous solubility, and hence the dissolution of the API. As we have seen in the previous section, diffusive molecular mobility in the amorphous state can vary by over many orders of magnitude as the temperature is changed; the relaxation times in the supercooled liquid from T_m to T_g can range from 10^{-12} to 10^2 s, respectively. Based on these values, samples stored at temperatures near or above T_g, clearly, would not have a sufficiently lowered molecular mobility to provide long-term storage, for example, 3 years, which represents a relaxation time on the order of 10^8 s. The goal, therefore, is to establish conditions

where either temperature T is lowered sufficiently to increase τ to something close to 10^8 s or T_g is raised relative to T with the addition of other amorphous solids having greater T_g values, as with API-polymer amorphous dispersions (to be discussed subsequently). It would also be beneficial if these other amorphous solids, such as polymers, could act as specific crystallization inhibitors.

Studies dealing with crystallization of organic molecules from the amorphous state in the absence of any solvent have shown that the classical picture of homogeneous nucleation and crystal growth from the liquid state can serve as a useful conceptual model [28]. Here, it is assumed that molecules in the liquid state under certain conditions must first undergo spontaneous nucleation, the formation of aggregates or nuclei consisting of a few hundred molecules, followed by the growth of macroscopic-size crystallites. The major thermodynamic factor driving nucleation and crystal growth is the free energy difference per unit volume between molecules in the amorphous state and those of the crystal, ΔG_v, as depicted in Figure 1.14. However, the formation of nuclei requires phase separation to occur with the creation of new surfaces between the nuclei and amorphous matrix, a process that is thermodynamically unfavorable. Because of this, when nuclei form there must be an increase in free energy ΔG_s, which for a spherical nucleus of radius r can be described as

$$\Delta G_s = 4\pi r^2 \sigma, \tag{1.11}$$

where σ is the surface free energy per unit area of surface (the surface tension in liquids) and $4\pi r^2$ is the surface area. Thus, the overall free energy of homogeneous nucleation,

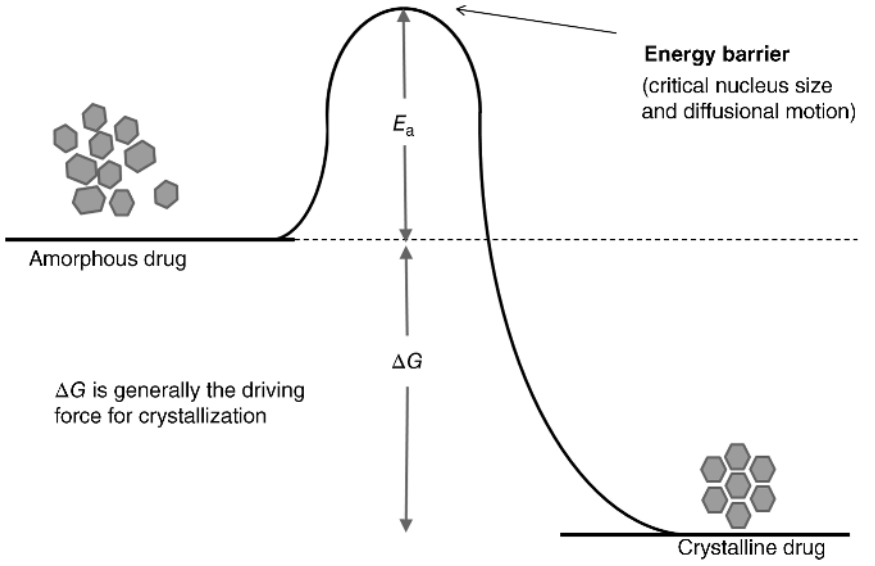

Figure 1.14. Schematic representation of the energetics associated with crystallization from the amorphous state.

ΔG^*, can be described by combining the two free energy terms, one favoring nucleation (ΔG_v) and the other opposing nucleation (ΔG_s):

$$\Delta G^* = \Delta G_v + \Delta G_s = (4/3)\pi r^3 \Delta G_v + 4\pi r^2 \sigma, \tag{1.12}$$

where $(4/3)\pi r^3$ is the volume of a sphere. It can be shown further, as illustrated in Figure 1.14, that the net change in ΔG^* will be positive until a critical radius r of nuclei is reached, above which the loss of free energy due to ΔG_V overcomes ΔG_s and spontaneous nucleation occurs. Thus, if specific nucleation inhibitors could be used to prevent the system from reaching the critical nucleus radius, further crystal growth could be avoided.

As has been implied throughout the discussion so far, an additional important free energy barrier to nucleation arises because of the decrease in diffusional molecular mobility that occurs as temperature is decreased. Expressing this kinetic energy barrier as $\Delta G'$, we can express the overall rate of nucleation, I, as

$$I \sim \exp(-\Delta G^*/kT) \exp(-\Delta G'/kT) \tag{1.13}$$

and can conclude, therefore, that as temperature is decreased (greater supercooling), the thermodynamic barriers to nucleation will decrease, while such cooling will increase the barriers to nucleation as molecular mobility is decreased. Similar analysis of thermodynamic and kinetic factors that affect the rate of crystal growth, u, once nucleation occurs, can be expressed as

$$u = D/\lambda[(1 - \exp(-\Delta G_v/kT)], \tag{1.14}$$

where D is the diffusion constant and λ is the jump distance across the growth interface. Thus, again we see the opposite effects of thermodynamic and kinetic energy requirements.

With this general conceptual picture of nucleation and crystal growth in mind, we can conclude that there are two major strategies that can be used to inhibit crystallization from the amorphous state: the addition of specific nucleation inhibitors, and/or the addition of molecules that will reduce the molecular mobility of the system at expected storage temperatures. In the first case, it should be possible to add molecules to the system that can accumulate at the site of nucleation and directly interact with the API thus interfering with nucleation. In the second case, it is important to first understand the temperature dependence of nucleation and crystal growth as illustrated by the temperature dependence for overall crystallization in Figure 1.15, where we see that the rates of both nucleation and crystal growth first increase with increasing temperature and then reach a maximum followed by a decrease [29]. It has also been suggested, as shown in Figure 1.15, that nucleation begins only when the temperature $T_{g\beta}$ associated with Johari–Goldstein β-relaxations is exceeded, thus providing a basis for the earlier suggestion that the β-relaxations are precursors to diffusive primary α-relaxations [26]. Earlier, it was also shown that $T_{g\beta}$ generally occurs at about 100 K below T_g and that α-motions become significant above 50 K below T_g. This means that strategies involving

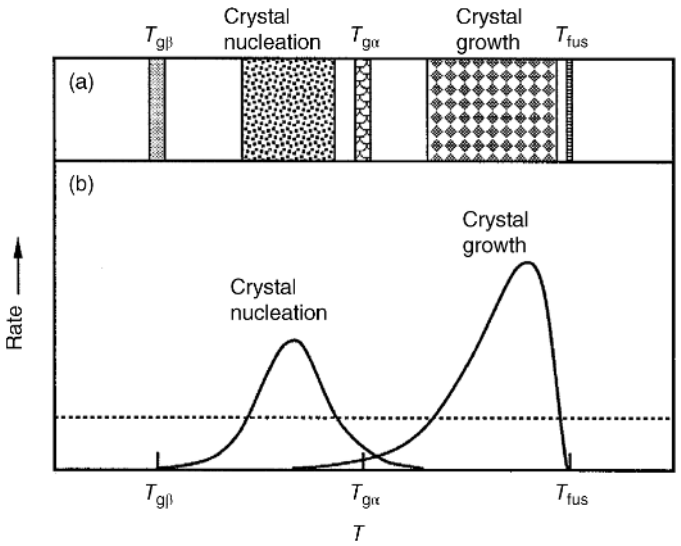

Figure 1.15. Rates of nucleation and crystal growth as a function of temperature in relationship to $T_{g\alpha}$ and $T_{g\beta}$ (reproduced with permission from Ref. 29. Copyright 1997, Elsevier).

a reduction in molecular mobility for inhibiting crystallization over long storage times should require $T_g - T$ to be somewhere in the range of 100–50 K.

1.6 SUPERSATURATION OF API IN AQUEOUS MEDIA FROM THE AMORPHOUS STATE

The major purpose of using the amorphous form of an API in solid dosage forms is to take advantage of the greater apparent solubility from the amorphous state relative to that from the crystal because of the lack of a well-ordered crystal lattice with attractive intermolecular energy that ordinarily tends to reduce solubility in the crystal. Three questions have to be addressed when taking this approach for enhancing API solubility: (i) Can the amorphous solid be maintained in the amorphous state over the time of storage before use? (ii) What level of improvement in solubility in aqueous media can be expected for the amorphous form relative to the crystal? (iii) Can the desired supersaturated concentration of dissolved API from the amorphous form be maintained over the time period required to ensure acceptable oral bioavailability? In the previous sections of this chapter, we have outlined a number of principles that allow the first question to be addressed. Here, we wish to examine the underlying principles that can be applied to address questions 2 and 3.

From a thermodynamic perspective, we would expect the relative solubility of a molecule in the amorphous and crystalline states at any temperature T to be directly determined by the free energy difference between the amorphous and crystalline forms, as illustrated in Figure 1.2. This free energy difference, designated as $\Delta G_T^{A/C}$, can be

expressed in terms of the activities of the molecule in the amorphous and crystalline states, a^{A} and a^{C}, respectively:

$$\Delta G_T^{\mathrm{A/C}} = RT \ln(a^A/a^C). \tag{1.15}$$

Assuming activity coefficients equal to 1, $\Delta G_T^{\mathrm{A/C}}$ can be expressed as

$$\Delta G_T^{\mathrm{A/C}} = RT \ln(c^A/c^C), \tag{1.16}$$

where c^{A} and c^{C} are the equilibrium solubilities of the API from the two solid forms. Consequently, knowing the equilibrium solubility of the API in water at temperature T, c^{C}, and the free energy change $\Delta G_T^{\mathrm{A/C}}$, one can estimate the expected value of c^{A}, the supersaturation concentration. One can experimentally determine $\Delta G_T^{A/\mathrm{C}}$ by recognizing that

$$\Delta G_T^{\mathrm{A/C}} = \Delta H_T^{A/\mathrm{C}} - T\Delta S_T^{A/\mathrm{C}}, \tag{1.17}$$

where $\Delta H_T^{A/\mathrm{C}}$ and $\Delta S_T^{A/\mathrm{C}}$ are the enthalpy and entropy differences between the amorphous and crystalline forms, respectively. Furthermore, it can be shown that

$$\Delta H_T^{A/\mathrm{C}} = \Delta H_T^C - (C_p^A - C_p^C)(T^C - T), \tag{1.18}$$

$$\Delta S_T^{A/\mathrm{C}} = \Delta S_T^C - (C_p^A - C_p^C)(\ln [T^C/T]), \tag{1.19}$$

and

$$\Delta S_T^C = \Delta H_T^C/T^C, \tag{1.20}$$

where T^{C} is the melting temperature of the crystal, ΔH_T^C is the heat of fusion of the crystal, ΔS_T^C is the entropy of fusion of the crystal, and C_p^A and C_p^C are the heat capacities of the amorphous and crystal forms, respectively. By experimentally measuring C_p^A and C_p^C using thermal analysis and T^{C} and c^{C} for the crystal at T, it is possible to use Equation 1.16 to predict the value of c^{A}, the apparent equilibrium solubility of the amorphous form that might be expected [30]. Recognizing that the activity of the amorphous solid can be reduced by the presence of any residual absorbed water and that many acidic and basic APIs can undergo some ionization in aqueous solution, a more rigorous thermodynamic expression to predict solubility of amorphous solids under such conditions has been reported [31]. As shown in Figure 1.16, the experimental maximum supersaturation level $c^{\mathrm{A}}/c^{\mathrm{C}}$ for indomethacin at 25 °C before the initiation of crystallization is about 4.9. Using Equation 1.16 the value predicted at 25 °C for indomethacin is on average about 29.0, while correcting for water absorption and ionization the value is reduced to 7.0, much closer to the experimental value of 4.9. Some uncertainty in the agreement between predicted and experimental values of $c^{\mathrm{A}}/c^{\mathrm{C}}$ comes from the fact that crystallization can be triggered by nucleation events that are not easily predicted and

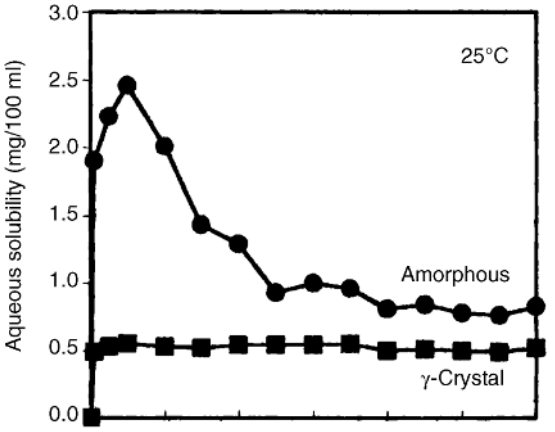

Figure 1.16. Solubility versus time for crystalline and amorphous indomethacin in water (reproduced with permission from Ref. 30. Copyright 2000, Springer).

reproduced. In a recent study, for example, the role of nucleation rates in determining levels of supersaturation of amorphous APIs upon dissolution has been modeled and analyzed by estimating the induction period for the initiation of nucleation and the appearance of crystals (time period for maintaining supersaturation) under various conditions [32].

1.7 MIXTURES OF AMORPHOUS SOLIDS

Mixtures of amorphous solids are of pharmaceutical interest when solid formulation ingredients undergo various types of processing that purposefully or inadvertently can lead to amorphous forms of two or more materials, for example, milling, compaction, drying, hot melt extrusion, and spray drying (see Figure 1.5). As we expect with simple liquids, mixtures of molecules in the amorphous state can exist as completely or partially separated phases, or as a single miscible phase. In the case of amorphous solid dispersions, which often consist of an amorphous mixture of API and polymer, a miscible amorphous system is generally required to obtain appropriate levels of stability, enhanced dissolution, and oral absorption. Consequently, it is important to review some of the underlying principles that determine the extent to which mixtures of different amorphous materials are miscible or immiscible. Of course it must be recognized that although amorphous components may be miscible, the system is still metastable relative to the crystalline forms of these components and eventually can undergo crystallization. We can first address this issue by applying some general thermodynamic principles related to the mixing of liquids. We begin by recognizing that for intermolecular mixing of liquids to occur, there must be an overall loss in the Gibbs free energy of mixing, ΔG_{mix}, at temperature T expressed as

$$\Delta G_{\text{mix}} = \Delta H_{\text{mix}} - T\Delta S_{\text{mix}}, \tag{1.21}$$

where ΔH_{mix} and ΔS_{mix} are the enthalpy and entropy of mixing, respectively. Generally, the mixing of different molecules leads to an increase in entropy, so that the positive entropic term in Equation 1.21 leads to a loss of free energy and the favoring of miscibility. On the other hand, if we consider the molecular mixing of two components A and B, ΔH_{mix} can be either negative or positive depending on the relative strength of the interactions between A:B and between A:A and B:B. Stronger A:B interactions lead to a loss in enthalpy, while stronger A:A and B:B interactions lead to an increase in enthalpy. Thus, the former will contribute to a loss in free energy, while the latter will contribute to an increase in free energy. We can generalize further by saying that two organic molecules having similar levels of polarity and, therefore, capable of undergoing significant intermolecular interaction, for example, hydrogen bonding, would be expected to produce miscible amorphous mixtures, while chemical incompatibility could lead to phase separation of the two or more amorphous forms if not offset by positive entropy changes. An example of such a system is that of amorphous citric acid (quite polar) and indomethacin (relatively hydrophobic) that phase separate beyond a certain concentration [33]. To gain a more quantitative understanding of those factors that control molecular mixing in the amorphous state, it would be desirable to have a theoretical framework that describes the free energy of mixing of liquids at a fundamental level in terms of measurable parameters. The Flory–Huggins lattice theory [34], presented in the Flory–Huggins equation, and originally developed for polymer solutions, describes the Gibbs free energy of mixing per mole for a polymer and a "solvent" as

$$\Delta G_{\text{mix}} = RT(n_A \ln \phi_{\text{A}} + n_B \ln \phi_{\text{B}} + n_A \phi_{\text{B}} \chi_{\text{AB}}), \tag{1.22}$$

where R is the gas constant, ϕ is the volume fraction of each component, χ is the interaction parameter that describes the tendency for interaction between the components A and B, and n is the number of moles of each component. The first two terms in the parenthesis represent the entropic contributions, while the third term represents the enthalpic contributions from intermolecular interactions. For the purposes of this discussion, component A will refer to the "solvent" and component B to the polymer. The smaller or more negative the interaction parameter, the stronger the intermolecular interaction between A and B. From a conceptual perspective, the Flory–Huggins equation is very useful in demonstrating the importance of molecular size in affecting miscibility through a reduction in the entropy of mixing. For example, in Equation 1.23, the entropy of mixing per mole can be described as

$$S_{\text{mix}} = -R(n_A \ln \phi_{\text{A}} + n_B \ln \phi_{\text{B}}). \tag{1.23}$$

If we now express the number of moles of each component in terms of the mass m and molecular weight M, we can rewrite Equation 1.23 as

$$\Delta S_{\text{mix}} = -R[(m_A/M_A) \ln \phi_{\text{A}}) + (m_B/M_B) \ln \phi_{\text{B}}]. \tag{1.24}$$

The important conclusion from this equation is that the greater the molecular weight of any component, the less the contribution of entropy to the free energy of mixing, and thus the

less the tendency for miscibility of the system. Essentially, by mixing two macromolecules that individually have many degrees of conformational freedom, any configurational entropy associated with this freedom will be reduced upon mixing and interaction of the two components. Consequently, we would expect that all other factors being equal the miscibility of amorphous binary systems involving at least one polymer would be reduced relative to those for two small molecules and that a mixture of two polymers would have a strong tendency to lose less free energy and possibly phase separate. Indeed, many amorphous polymer blends exhibit significant immiscibility for this reason.

To further examine the thermodynamics of mixing in amorphous solids and the possible relationships with the structural features of the amorphous state, for example, molar volume or density, it will be useful to consider the volumetric changes that can occur with the mixing of components having molar volumes of V_A and V_B. First, recall that the volume per molecule or mole of any component X at any temperature is determined by the volume occupied by the mass of a molecule, V_{occup}, plus any free volume V_{free} that exists between the molecules, as determined by the degree and nature of the molecular packing, as expressed in Equation 1.25:

$$V_X = V_{occup} + V_{free}. \tag{1.25}$$

Consequently, when two molecules A and B are mixed, the net volume change will have contributions from both their occupied and free volumes in proportion to the volume fraction of each of the individual components; as temperature is changed, these volumetric changes will be strongly affected by changes in V_{free}. For an ideal solution, where ΔH_{mix} is equal to zero, we would expect that the volume of the mixture, V_{AB}, would be the sum of the weighted average of the molar volume of each component:

$$V_{AB} = n_A V_A + n_B V_B, \tag{1.26}$$

where V_A and V_B are the molar volumes and n_A and n_B are the mole fractions of components A and B, respectively. This means that for ideal mixing, the occupied and free volumes of each component will be additive in a manner weighted exactly by each component's mole fraction. From the thermodynamic analysis described above, it would be expected that miscible mixtures of amorphous solids, where ΔH_{mix} is not equal to zero, will exhibit nonideal mixing so that there would be an excess molar volume change, V_{excess}, that can be either positive or negative depending on the nature of the intermolecular interactions giving rise to an enthalpy change. In such a case V_{AB} can be written as

$$V_{AB} + n_A V_A + n_B V_B + V_{excess}, \tag{1.27}$$

where very strong interactions between A and B lead to a negative excess volume, that is, a reduction in overall volume, as in the well-known case of the mixing of ethanol and water, while stronger interactions between A and A and B and B than between A and B lead to a positive excess molar volume or an increase in overall molar volume.

From Equation 1.27 and our previous discussion of factors that might influence the glass transition temperature of any amorphous solid, it would appear that the various

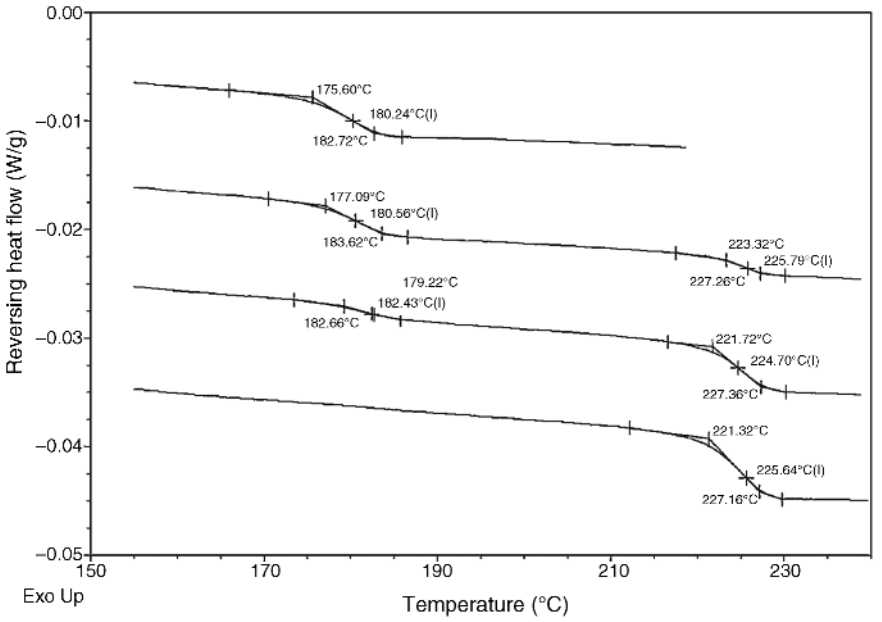

Figure 1.17. Overlay of modulated DSC, reversing heat flow, from top to bottom: PVP, 70 and 30 wt% dextran in PVP dispersions, and dextran (Mn: 64–76 kDa) prepared by freeze-drying (reproduced with permission from Ref. 35. Copyright 2008, Wiley-Liss, Inc).

volumetric changes taking place in the formation of a miscible amorphous mixture, as discussed above, would be reflected in a single value of T_{gmix} intermediate to the values of the individual components. On the other hand, if the two components are immiscible, we would expect there to be two values of T_g equal to the values of the pure individual components. For example, in Figure 1.17, we can observe two values of T_g for a mixture of PVP and dextran, prepared by freeze-drying from an aqueous solution of both components [35]. Note that the values are equal to the T_g of each pure component at all concentrations, indicating complete phase separation. In contrast, consider Figure 1.18 that indicates the values of T_g for pure amorphous indomethacin and PVP, as well as for two mixtures of indomethacin and PVP with different concentrations. Here, we can see that at each concentration there is only one T_g (T_{gmix}) that tends to increase as the concentration of the component having the greater T_g is increased, thus indicating a miscible mixture. Recognizing that it is important to establish the absence or presence of miscibility in amorphous solid dispersions, it would be important to examine some issues related to determining miscibility in amorphous mixtures. As has already been inferred, completely miscible amorphous systems should exhibit a single T_g intermediate to the individual values and dependent on the concentration of components. Typically, DSC measurements, which reflect thermal changes associated with changes in molecular mobility, are not able to produce distinctly separate values of T_g if the T_g values of the individual components are closer than about 10 K, and if the phases that separate have dimensions on the order of $<$100 nm. Thus, conditions that might lead to nanosized clusters of separated components

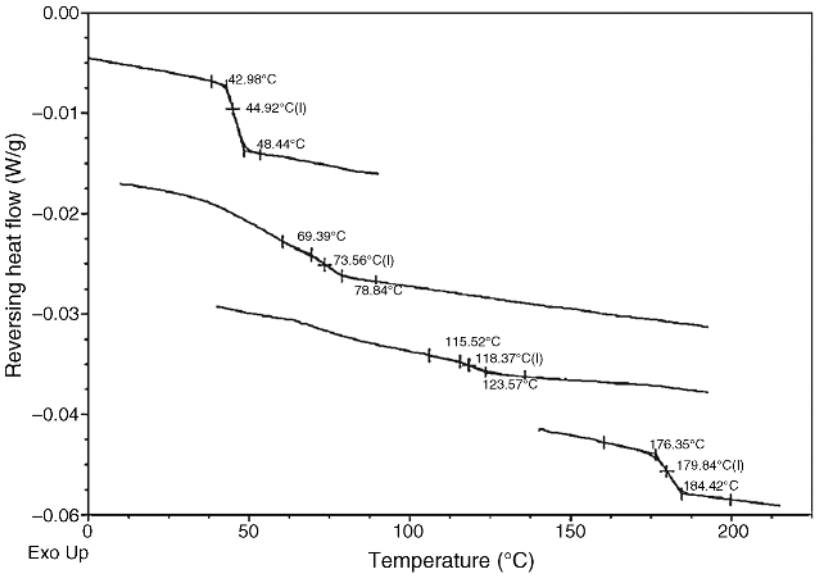

Figure 1.18. Overlay of modulated DSC, reversing heat flow, from top to bottom: indomethacin prepared by melt quench, 70 and 30 wt% indomethacin in PVP dispersions and PVP prepared by flash evaporation (Reproduced with permission from Ref. 35. Copyright 2008, Wiley-Liss, Inc).

would produce a DSC thermal response that indicates only one T_{gmix}. To further establish whether amorphous mixtures truly exist in a single phase, it is possible to use PXRD measurements, as well as SSNMR spectroscopy, since both techniques probe molecular interactions at a very local level. For example, in the case of PXRD, one can compare diffraction patterns of the amorphous mixture with those of the individual components, and if the sum of the weighted average of the patterns of the individual components is the same as that of the mixture, the system is completely phase separated [35]. If the calculated values for the mixture do not coincide with those experimentally determined, the system can be considered to exist as a single phase. One also can determine the PDF of the individual components and the mixture, and similarly compare the sum of the weighted average of the PDFs of the components with that of the mixture. Again, if the weighted average of the PDFs of the individual components is the same as that of the mixture, the system is immiscible, whereas differences indicate miscibility [35]. It is also possible to use solid-state NMR to detect phase separation down to domain sizes less than 100 nm using two-dimensional NMR [36] and by measuring T_1 and $T_{1\beta}$ relaxation times that respond to NN and NNN distance interactions between components. For example, it was recently shown that a lyophilized amorphous mixture of trehalose and dextran produced a single T_g that changed with the concentration of the components. However, PDF analysis of these mixtures, as described above, revealed complete phase separation [35]. SSNMR analysis of this system revealed, indeed, that separate molecular clusters with dimensions on the order of 55–80 nm could be detected [37].

It would be of further interest to know *a priori* how T_{gmix} might change with concentration so that rough predictions might be made by only knowing the individual values of T_{g}. To see how this might be done, we can start with ideal mixing, as described in Equation 1.26, to show that

$$T_{\text{gmix}} = \phi_{\text{A}} T_{\text{g A}} + \phi_{\text{B}} T_{\text{g B}}, \tag{1.28}$$

where ϕ_{A} and ϕ_{B} are the volume fractions of components A and B, respectively. For such ideal mixing, we assume that the free volume of the mixture is simply the sum of the free volumes of the individual components. Typically, when working with mixtures of amorphous solids, the concentration of the various ingredients is expressed as weight fraction w rather than volume fraction. Consequently, as shown by Gordon and Taylor [38], Equation 1.28 can be expressed in terms of weight fraction as

$$T_{\text{gmix}} = [(w_A T_{\text{g A}} + w_B T_{\text{g B}})/(w_A + K w_{\text{B}})], \tag{1.29}$$

where for ideal mixing

$$K = [(\rho_{\text{A}} T_{\text{g A}})/(\rho_{\text{B}} T_{\text{g B}})], \tag{1.30}$$

where ρ is the density of each component at its respective T_{g}. The same general equation for ideal mixing, as described in Equation 1.29, has been derived on a thermodynamic basis by Couchman and Karasz [39], with K now defined in terms of the heat capacity changes taking place at T_{g} for each individual component:

$$K = \Delta C_{p\text{A}} / \Delta C_{p\text{B}}. \tag{1.31}$$

It can be further shown that when the densities of the two components are very similar, as in the case of many polymers, Equations 1.29 and 1.30 lead to the Fox equation [40], where

$$1/T_{\text{gmix}} = [(w_A/T_{\text{g A}}) + (w_B/T_{\text{g B}})]. \tag{1.32}$$

Further estimations of T_{gmix} for ideal mixing in systems containing more than two amorphous components, for example, API, polymer, and water, although more complex and uncertain, can be carried out as extensions of Equation 1.29 or Equation 1.32 [41,42]. The simplest approach for a system containing n components using an extension of Equation 1.32 would be

$$1/T_{\text{gmix}} = [(w_1/T_{g1}) + (w_2/T_{\text{g2}}) \cdots (w_n/T_{\text{g}\,n})]. \tag{1.33}$$

Despite the strong possibility of nonideal mixing in most practical systems encountered, these equations for ideal mixing can be useful for estimating the glass transition temperature of a miscible mixture of amorphous components for a number of reasons. Initially, one may want to get a rough estimate of what composition of polymer and API

might be required to provide a certain value of T_{gmix}, given only the individual T_g values. This can be done very simply by using Equation 1.32 or Equation 1.33 or by estimating K in Equation 1.30 or Equation 1.31 and using Equation 1.29. To test for ideality or nonideality in the amorphous mixture, one can use these estimates of T_{gmix} and experimentally determine T_{gmix}. Deviations of experimental results from the expected plot would indicate that the mixing of components is nonideal; the deviations can be either negative or positive, meaning that the experimentally determined values of T_{gmix} are either greater or less than predicted. Values greater than those predicted for ideality indicate that the net excess free volume is less than that expected for the weighted sum of individual component free volumes, or that A:B interactions are greater than the A:A and B:B interactions. If the deviations are negative, this means that there is greater excess free volume than expected or stronger A:A and B:B interactions than those between A and B. Examples of T_g versus concentration profiles for ideal and nonideal mixtures with positive and negative deviations from ideality in miscible amorphous mixtures have been reported for pharmaceutical systems [43–45].

1.8 FORMATION AND PROPERTIES OF AMORPHOUS SOLID DISPERSIONS

The focus of the remaining parts of this chapter, and indeed, the rest of this book, will be on amorphous solid dispersions, which we will define as single-phase amorphous mixtures of an API and water-soluble polymer intended to produce enhanced aqueous dissolution and oral bioavailability [46]. The polymer is used (i) to provide long-term storage stability of the amorphous API by inhibiting solid-state crystallization and (ii) to maintain a desirable level of supersaturation in the dissolution medium by preventing solvent-mediated crystallization over the time period needed for the required bioavailability. In some cases a surfactant is included in an ASD to further promote dissolution and/or to facilitate the manufacturing process. Various details of the processing of amorphous dispersions and the ingredients used on a practical scale will be discussed throughout this book. Here, we wish to introduce some general concepts and issues that build on the principles discussed above. Depending on the physical and chemical characteristics of the API and polymer, amorphous solid dispersions are primarily prepared by either hot melt extrusion (HME) of a mixture of powdered API and polymer, or by the spray drying of a solution of API and polymer from a suitable volatile solvent. In HME the dry powder mixture is placed into an extruder at elevated temperatures that melts or softens the components to facilitate mixing. The material is continuously extruded, cooled, and chopped into small fragments, often called lentils, which are further milled with other formulation ingredients into powdered form. Ideally, to facilitate the process of molecular mixing, the crystalline API should be melted, if it is not prone to chemical decomposition at these elevated temperatures, and the polymer should have as low a T_g as possible to promote softening at these temperatures. Surfactants, such as those tabulated in Appendix A, are often added to lower melting and glass transition temperatures. Advantages of the HME process are that it can be carried out continuously, is solvent-free, and can be scaled up to

large-scale manufacturing. Spray drying generally involves the spraying of a suitable solution of API and polymer into a heated chamber under tight control of droplet size, spray rate, and other process variables, followed by the rapid evaporation of the solvent and precipitation of the remaining solids to form the amorphous dispersion. Special consideration in the drying process is given to the solubility characteristics of the API and polymer so that miscibility is ensured and maintained as drying occurs. A wide range of solvents and solvent mixtures with varying polarity provide flexibility in the control of the drying process. Spray drying has the additional advantages of being easily scaled up for manufacturing and of providing a means of producing well-controlled particle sizes.

The major polymers used to prepare amorphous solid dispersions are either water soluble under all pH conditions or enteric coating polymers that contain acidic groups that ionize at higher pH values to become water soluble. The most widely used polymers include vinyl-pyrrolidone-based polymers, such as poly(vinyl pyrrolidone) (PVP) and the poly(vinyl pyrrolidone)-poly (vinyl acetate) copolymer (PVP-VA); cellulose-based polymers such as hydroxypropyl methylcellulose (HPMC) and hydroxyl propyl methylcellulose acetate-succinate; and methacrylate-based enteric coating polymer systems such as the Eudragits. The monographs in Chapter 14 and the Appendix A tables list various grades of these and other useful polymers with their corresponding T_g values. Generally speaking, polymer grades that have lower T_g values, for example, in the range of 100 °C, appear to be most useful in the HME process that requires that the ingredients be melted and/or softened to facilitate mixing. It is important to keep in mind that an ASD itself is only an extension of the API and that it must be further formulated and processed to produce a stable and effective oral solid dosage form. Consequently, an important initial goal is to produce an ASD that contains a minimum amount of polymer so that the required "dose" of the API–polymer combination does not become so excessive that it impacts the size of the dosage unit and influences the types and amounts of the other excipients required to ensure proper manufacturing and performance. This minimization of the amount of polymer must be measured, of course, against the primary role of the polymer as an inhibitor of solid-state and solvent-mediated crystallization.

Central to the functioning of a polymer in an ASD is the formation of a single-phase "miscible" system. As already described, the mixing tendencies of amorphous materials are governed by the same general thermodynamic principles that operate with the mixing of liquids. Thus, the concentration of components, their molecular size and shape, and their degree of polarity and ability to interact are all critical characteristics that must be evaluated in choosing an appropriate API–polymer combination. Typically, for simple liquids, miscibility is taken as the mutual *equilibrium solubility* of the components, determined experimentally in terms of concentration and temperature by the establishment of characteristic phase diagrams, which represent well-defined relationships between regions of miscibility and immiscibility. In dealing with mixtures of amorphous materials, prepared by processes that tend to produce metastable states, that is, melting or drying, we can expect most often that the API concentration will be greater than that representing the true equilibrium solubility of the crystalline API in the polymer, and hence still thermodynamically prone to eventual crystallization. If the amount of API is low enough, it is possible that a dispersion can be prepared at a level of API below the equilibrium solubility

of the crystal, thus producing both kinetic and thermodynamic solubilities of the system. Recent studies have described a thermal method of measuring the equilibrium solubility of crystal drugs in various polymers, and have shown that these equilibrium solubilities are generally quite low, suggesting that most practical amorphous solid dispersions with the usual therapeutic dose ranges represent metastable solutions of API in polymer [47]. Thus, it is critical that consideration be given to how one can maintain the physical stability of amorphous API for periods required during the storage of the solid dosage form.

1.9 SOLID-STATE CRYSTALLIZATION FROM AMORPHOUS DISPERSIONS

We have already mentioned that the critical steps in preventing solid-state crystallization of an amorphous API are (i) inhibition of nucleation and crystal growth rates by reducing molecular mobility of the API, and (ii) direct interaction of a nucleation inhibitor with the API. The term direct interaction is used here since the formation of any miscible amorphous dispersion generally requires interaction between the API and polymer, most often through hydrogen bonding, whereas inhibition of nucleation requires interaction of the polymer with the specific functional groups on the API that are critical for nucleation. From the previous discussion of the amorphous state and amorphous mixtures, and Equation 1.32, we can now see, in practical terms, how an amorphous excipient with a high T_g and sufficient miscibility with an API would be able to produce relatively high values of T_{gmix}, compared with the T_g of the API alone, and hence reduce the molecular mobility of the API when stored at a particular temperature. Such a decrease in molecular mobility of the API in turn might be enough to reduce tendencies for crystallization of the API under the normally required storage conditions of 2–3 years. For example, if an amorphous API has a T_g value of 320 K (47 °C), alone, it would have to be stored near 0 °C to be at $T_g - T$ equal to at least about 50 K, roughly the temperature range where diffusive molecular mobility is reduced to time periods suitable for preventing crystallization during storage over a few years. To store a sample of this API at 25 °C for a few years without crystallization, for example, one would need to raise the T_g of the system to about 75 °C (348 K) or higher, which according to Equation 1.32, and the individual T_g values would require a minimum of about 30% w/w of a miscible polymer having a T_g of 150 °C (423 K). To store the sample at 40 °C (313 K) for a few years, one would have to raise the T_g to roughly 90 °C (363 K) by using about 50% w/w of this polymer. Figure 1.19 presents experimental studies of the percent of crystallization at 30 °C of amorphous indomethacin with a T_g of 42 °C (315 K) alone and mixed with PVPK90, having an average molecular weight of about 1.5 million and a T_g of 180 °C (453 K) [43]. Here, it can be observed that physical mixtures of the amorphous indomethacin and PVP containing 5% w/w PVP exhibit identical rates of crystallization with indomethacin alone. Such behavior was also observed at all concentrations up to 90% w/w PVP. Note in Figure 1.19 that only 5% w/w PVP in the form of a miscible mixture prevents any crystallization up to a period of 6 months, indicating a significant reduction in the rate of nucleation and crystal growth. It was shown further that increasing the amount of polymer in the dispersion to 30% w/w PVP prevented crystallization for over 2 years.

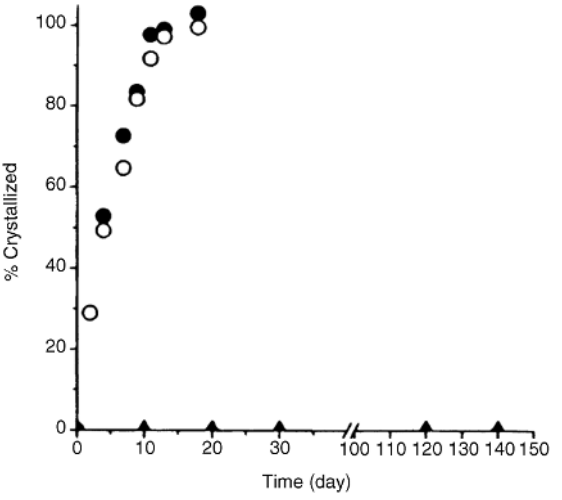

Figure 1.19. Percent crystallization of indomethacin from the amorphous state at 30 °C: alone (dark circles); physically mixed with 5%PVP (open circles); miscible amorphous mixture with 5% PVP (dark triangles) (reproduced with permission from Ref. 43. Copyright 1999, Springer).

Interestingly, whereas the 30% w/w PVP dispersion has a T_g of 61 °C (334 K) so that at 30 °C (303 K) $T_g - T$ is equal to 31 K, 5% w/w PVP with a T_g of 47 °C (320 K) has a $T_g - T$ of 17 K not very different from indomethacin alone with a $T_g - T$ of 12 K. Thus, it appears that the hypothetical analysis and predictions concerning $T_g - T$ and crystallization, presented above using Equation 1.32, are quite reasonable for the 30% w/w dispersion, while PVP at the 5% w/w level is much more effective than might be predicted from effects on molecular mobility alone. Indeed, others have shown that even at levels of 1–2% polymer in a miscible dispersion, there can be significant inhibition of crystallization [48,49] even though there is a negligible increase in T_g over that of the API alone. In the case of 5% w/w dispersions of indomethacin–PVP, evidence from FTIR measurements indicates that PVP interferes through hydrogen bonding with the dimer formation in amorphous indomethacin that is required to initiate nucleation, whereas no such indomethacin hydrogen bonding is observed in the physical mixture [48]. That the 30% w/w PVP dispersion was so effective with a $T_g - T$ of only 31 K, rather than 50 K, further suggests a more specific direct interaction at nucleation sites that contribute to the inhibition of crystallization. We can conclude, therefore, that the inhibition of solid-state crystallization of amorphous API by polymers in an ASD is generally governed by direct interactions that prevent nucleation and by decreasing molecular mobility, that is, increasing diffusive α-relaxation times, and likely increasing secondary β-relaxation times that serve as precursors to the onset of diffusional motions.

Up to this point the ASD systems discussed have been assumed to be essentially free of any water taken up from the atmosphere. Consequently, all T_g values, relaxation times, and quantitative estimations or predictions were made using parameters established for the "dry" API and polymer. Generally, however, when an amorphous solid is exposed to elevated relative humidity (RH), the solid tends to absorb the water vapor into its bulk structure and form a miscible amorphous mixture [50]. The amount of water taken up at a particular RH and temperature will be greater with an increase in degree of polarity of the

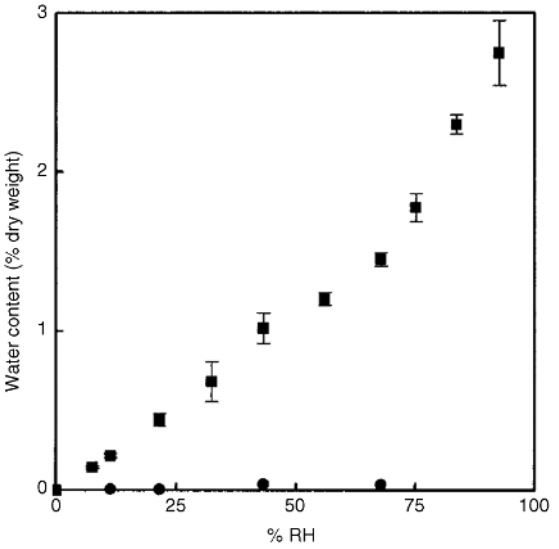

Figure 1.20. Water vapor absorption by amorphous (squares) and crystalline (circles) indomethacin at 30 °C as a function of relative humidity (reproduced with permission from Ref. 52. Copyright 1997, John Wiley & Sons, Inc.).

solid. This is in contrast to water uptake by crystalline solids where water molecules are generally confined to the surface, rarely reaching more than 0.1% w/w adsorbed, or the equivalent of 3–4 molecular layers, even for very polar solids such as NaCl [51]. The relationship between the amount of water vapor absorbed and RH at a particular temperature can be analyzed by determining a water sorption isotherm, as shown for amorphous indomethacin in Figure 1.20 [52], and for three widely used polymers PVP, HPMC, and HPMCAS in Figure 1.21 [53]. Note that the amount of water absorbed at 30 °C by the relatively hydrophobic indomethacin molecule is quite small, for example,

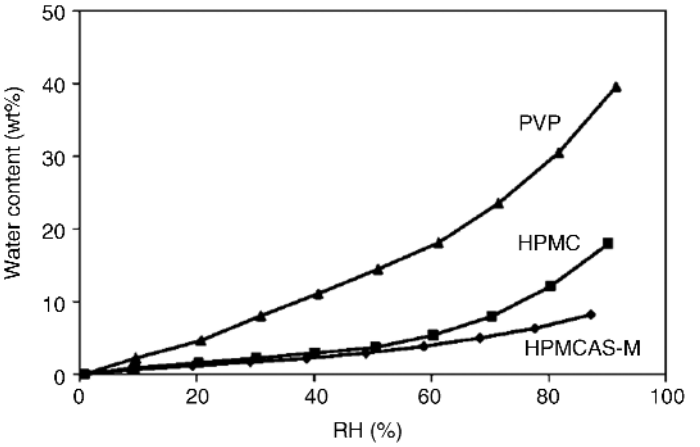

Figure 1.21. Water vapor absorption by three amorphous polymers varying in polarity (reproduced with permission from Ref. 53. Copyright 2008, American Chemical Society).

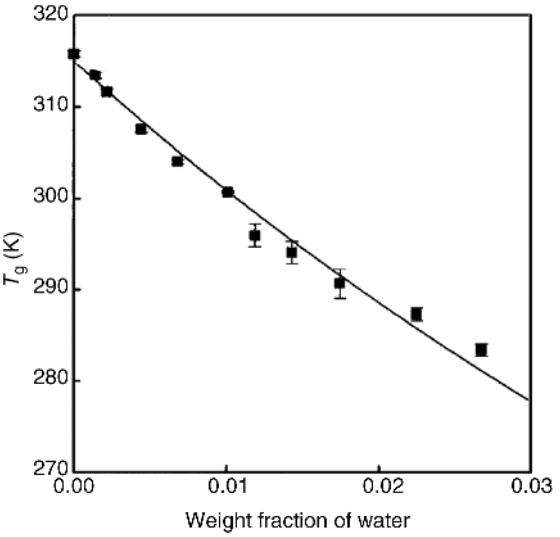

Figure 1.22. Glass transition temperature of amorphous indomethacin as a function of water content (reproduced with permission from Ref. 52. Copyright 1997, John Wiley & Sons, Inc.).

about 1% w/w at 50% RH and 2% w/w at 83% RH, whereas water vapor absorption at room temperature by PVP, HPMC, and HPMCAS at 75% RH is about 26% w/w, 10% w/w, and 7% w/w, respectively. These results are consistent with the general order of polarity and hydrogen bonding ability of these polymers. What they also indicate is that most of the water that is absorbed by a typical API–polymer dispersion would be expected to be associated with the polymer. This is a reasonable generalization since amorphous dispersions are prepared because the API is usually somewhat hydrophobic. Water absorbed into an amorphous solid would be expected to have an effect on the bulk properties of the solid, for example, T_g and molecular mobility, as can be seen in Figure 1.22, where T_g is plotted versus water content for amorphous indomethacin. Here, we can see that in both cases water acts to reduce T_g very significantly, acting as an excellent plasticizer. Such plasticizing effects can be roughly predicted for any water content by applying Equation 1.32 and using the values of 136, 315, and 453 K for the T_g of water, indomethacin, and PVP, respectively. Consider, first, a situation where indomethacin alone is exposed to an environment at 40 °C and 75% RH, resulting in a concentration of water in the API of about 1.7% w/w. From the application of Equation 1.32, it can be shown that T_g would be reduced from 315 to about 308 K, whereas storage of PVP at 40 °C and 75% RH, with 26% w/w water being absorbed, leads to a reduction of the T_g of PVP from 453 to 282 K. Such a significant reduction in T_g close to 0 °C (273 K) would clearly create significant mobility at 40 °C where the sample is stored at 31 K above the new T_g of PVP in the supercooled liquid state. One might mitigate this result to some extent by choosing to use a less polar polymer such as HPMC that has a dry T_g of about 175 °C (448 K) and absorbs 10% w/w water at 75% RH. From Equation 1.31 we can calculate that the T_g of HPMC in the presence of 10% w/w water would be reduced to 364 K, and therefore when stored at 40 °C it would be 52 K below T_g in the glassy state, a much better solution for preventing crystallization in the hydrated

API dispersion. To observe the trade-off between the dry T_g of the polymer and its ability to absorb water, let us finally consider HPMCAS, which has a "dry" T_g of about 115 °C (388 K), and, as shown above, the ability to absorb about 7% w/w water at 75% RH. From Equation 1.32 we would estimate that T_g for HPMCAS with 7% w/w water content would be reduced from 448 K to 344 K, so that at 40 °C, the sample of HPMCAS would have a T_g that is 30 K above the new T_g, a better result than when using PVP that takes up considerably more water. Because of the lower T_g of HPMCAS compared with HPMC, however, this system is still in the supercooled liquid, which indicates the importance of reducing water content to very low values. The fact that HPMCAS is very widely used to form API amorphous dispersions, as will be seen throughout this book, indicates that HPMCAS most likely must also function as a stabilizer by being able to more directly interact with the API and interfere with nucleation. In conclusion, this discussion generally suggests a strategy for storing amorphous solids for long periods without crystallization that includes (i) using polymers with relatively high T_g; (ii) using as high a concentration of polymer in the dispersion as is possible without introducing other negative factors; (iii) using polymers that tend to absorb less water than PVP (see Figure 1.21); (iv) limiting exposure of the dispersion and solid formulation to humid atmospheres by proper processing conditions and packaging; and (v) if possible, including specific nucleation inhibitors that would not adversely increase molecular mobility. Clearly, removal of as much absorbed water as possible is critical.

1.10 DISSOLUTION AND SUPERSATURATION OF API FROM AMORPHOUS SOLID DISPERSIONS

Clearly, the main purpose of using amorphous forms of an API in solid dosage forms is to enhance its dissolution rate and oral bioavailability when the crystalline form cannot be used for such purposes. As shown in Figure 1.16, upon contacting the aqueous dissolution media, the API generally dissolves rapidly and reaches some level of supersaturation primarily determined by the free energy difference between the amorphous and crystalline forms. Upon attaining a certain level of supersaturation in the aqueous phase, the API molecules will generally undergo solvent-mediated nucleation and crystal growth, thus depleting the solution of dissolved API and reducing the solubility advantage sought with such systems; the greater the level of supersaturation attained, the greater the rate of nucleation and the shorter the time period over which supersaturation levels can be maintained. If the rate of dissolution of the added amorphous API, upon contact with the aqueous medium, is slow relative to solid-state crystallization rates, it is also possible that solid API would undergo crystallization due to the plasticizing effects of the water and not attain significant supersaturation because of reduced amounts of amorphous API. As we have already seen, many polymers can form amorphous dispersions with an API and significantly inhibit solid-state crystallization by reducing molecular mobility and by direct interaction at nucleation sites. Consequently, if there is no significant slowing down of the dissolution of the API and polymer when they make contact with the dissolution medium, there will likely be sufficient inhibition of solid-state crystallization to allow the API and polymer to readily dissolve and reach high levels of supersaturation. Having seen that the

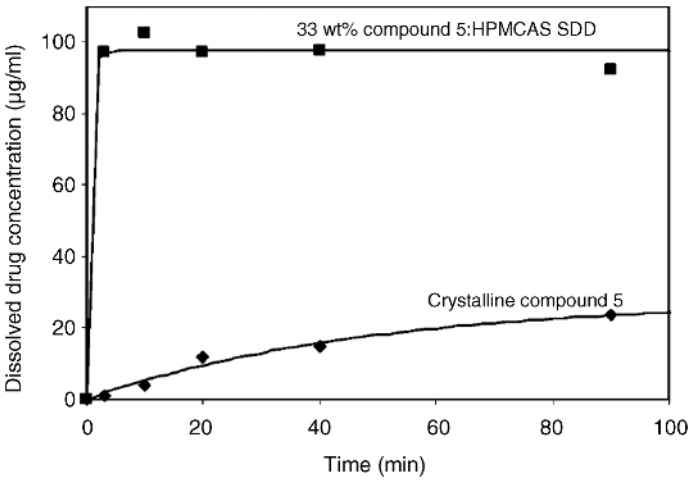

Figure 1.23. Comparison of dissolution rates and levels of supersaturation for a crystalline compound and its amorphous dispersion with HPMCAS (reproduced with permission from Ref. 53. Copyright 2008, American Chemical Society).

formation of API–polymer amorphous dispersions can greatly inhibit solid-state crystallization during storage even at low polymer concentrations, and that the best polymers in this regard tend to directly interact with the API through hydrogen bonding [48], it seems likely that such polymers could also inhibit solvent-mediated crystallization after dissolution of the API and polymer by such interactions in solution. A number of studies, indeed, have shown that polymers, such as PVP, HPMC, and HPMCAS, added to an aqueous solution at solution concentrations that might be expected from a typical API–polymer dispersion significantly inhibit nucleation, decrease the rate of crystal growth, and maintain high levels of supersaturation over extended periods of time [54,55]. That this actually occurs with the dissolution of API–polymer dispersion is illustrated in Figure 1.23 [53]. Recently, increasing evidence has been accumulated to suggest that supersaturation levels of API administered as API–polymer amorphous dispersions can be maintained at high levels by additional possible mechanisms. For example, as illustrated in Figure 1.24, it has been suggested that API–HPMCAS systems upon contact with a dissolution medium initially precipitate as complex high-energy colloidal noncrystalline phases that can retard crystallization and produce a high degree of supersaturation [53]. This behavior has been attributed to the relatively hydrophobic and surfactant-like nature of HPMCAS, and in this regard it has also been suggested that it is likely that such colloidal systems form during *in vivo* dissolution by interacting with colloid forming gastrointestinal materials such as fatty acid derivatives and bile salts. It has also been recently shown that a relatively hydrophobic API, ritonavir, in PVP dispersion at high levels of supersaturation can phase separate as a colloidal API-rich liquid phase that resists crystallization and maintains high levels of supersaturation [56]. Greater detailed discussion of all of these principles related to the inhibition of solid-state

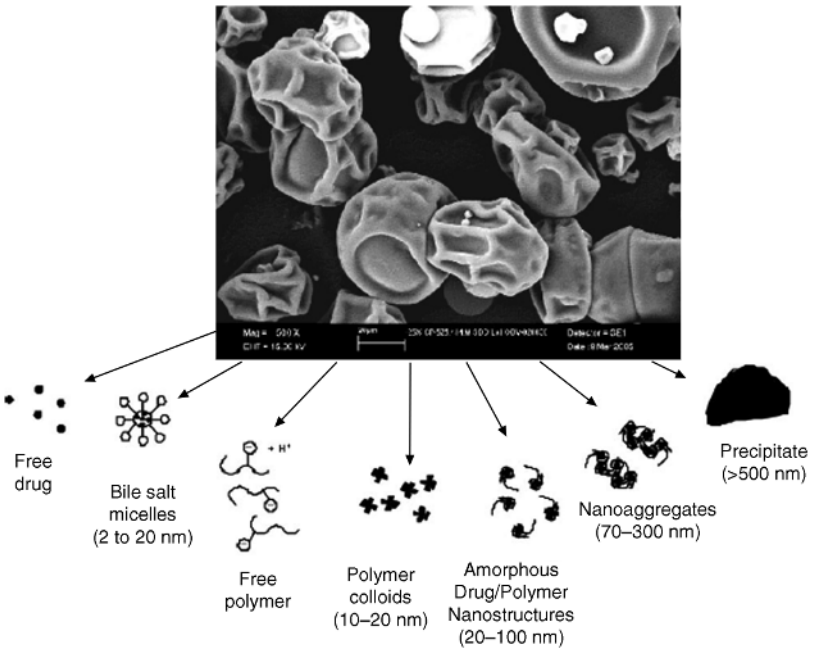

Figure 1.24. Species that can form when HPMCAS solid dispersions are added to aqueous solutions simulating duodenal and intestinal contents (reproduced with permission from Ref. 53. Copyright 2008, American Chemical Society).

and solvent-mediated crystallization during dissolution, including choice of polymers, surfactants, and processes, will be presented in later chapters.

1.11 PHARMACEUTICAL DEVELOPMENT OF AMORPHOUS SOLID DISPERSIONS

Once it has been decided that an ASD will be moved forward, a number of factors need to be considered during the development process. Many scientists consider an ASD as a "formulation" that is then processed into a usable dosage form. Another way to view an ASD is as another solid form. When considered as another solid form, the characterization and property assessment is similar to what has been performed previously for amorphous or crystalline APIs. Factors such as solubility, stability, excipient compatibility, handling, storage, performance, and developability all need to be considered. It is important to outline the critical properties that the dispersion needs to demonstrate in order to produce a successful drug product, and these properties can be used as selection criteria to find the best ASD.

Amorphous solid dispersions have their challenges, such as miscibility, stability, and hygroscopicity, but all of these can be overcome with careful consideration of

manufacturing, handling, and downstream processing. Understanding the limits of the ASD and incorporating these limits into the development plan are key decision points during development of these materials.

For early development projects, an ASD may provide the initial solubility boost needed to show proof of concept in a very simple formulation. It may be easy to overcome the challenges of a nonideal ASD for small-scale clinical trials, but these same issues may be insurmountable when moving to large-scale clinical batches. At that point, it must be decided if there is another dispersion available with better properties that can be moved forward or if there is a crystalline alternative that may now produce the needed performance based on the initial pharmacokinetic or metabolism studies. A change in solid form during the development process is a common occurrence as procedures are streamlined in early development to reduce costs and time. Once a drug has proven its worth, a more extensive look at possible forms and dosage forms takes place to find viable alternatives for late stage development. As with any solid form selection, the ASD with all the ideal properties may not be available, but a solid with most of the critical properties can be found and the noncritical properties can be dealt with via other methods, such as processing, formulation, packaging, and the like.

The goal of this book is to outline the various stages of producing, choosing, testing, formulating, and developing ASDs. Polymers and surfactants are necessary components of the dispersion and it is important to have an understanding of polymer properties when dealing with ASD projects. This will also help facilitate which polymers to include in a dispersion screen and the screening methods employed to produce possible dispersions. Chapters on characterization, stability, dissolution, and solubility will provide guidelines on dispersion properties that can be used to select a dispersion for early or late development. Choosing a manufacturing method, usually spray drying or melt extrusion, requires a knowledge of the properties needed for formulating the drug product as well as a comparison with material produced from small-scale processes used in initial studies to ensure that comparable properties are obtained for all materials.

The next phase involves using the ASD in various development activities such as formulation development (early or late) and preclinical/clinical studies. Early formulation development may employ a very simple or streamlined drug product to get an initial assessment of performance. Late-stage formulation development needs to cover a wide range of issues related to large-scale processing, packaging, storage, and use. Early preclinical studies are centered around proof of concept and bioavailability, while clinical studies need to deal with safety, efficacy, and performance of the API. At any stage, the ASD may need to be modified or replaced to move development forward.

It is also important to understand the regulatory components and requirements for dispersions. These include both manufacturing and testing of the dispersion and the final drug product. Information included in early versus late filings will be different and dependent on a number of factors related to the dispersion, API, and formulation. All dispersions found during development can be patented and patent strategies for

dispersions are critical for development and life cycle management over the life of the product.

This book will provide information and general strategies that can be used to develop drug products containing ASDs. However, every compound is unique and scientific rigor and understanding will be needed to put together the best development plan to successfully incorporate amorphous solid dispersions in drug products.

REFERENCES

1. Noyes, A.A. and Whitney, W.R. (1897) The rate of solution of solid substances in their own solutions. *J. Am. Chem. Soc.*, 54:930–934.
2. Amidon, G.L., Lennernas, H., Shah, V.P., and Crison, J.R. (1995) A theoretical basis for a biopharmaceutical drug classification: the correlation of *in vitro* drug product dissolution and *in vivo* bioavailability. *Pharm. Res.*, 12:413–420.
3. Hancock, B.C. and Shamblin, S.L. (2001) Molecular mobility of amorphous pharmaceuticals using differential scanning calorimetry. *Thermochim. Acta*, 380:95–107.
4. Lee, W.A. and Knight, G.J. (1970) Ratio of the glass transition temperature to the melting point in polymers. *Br. Polym. J.*, 2:73–80.
5. Fukuoka, E., Makita, M., and Yamamura, S. (1989) Glassy state of pharmaceuticals. III. Thermal properties and stability of glassy pharmaceuticals. *Chem. Pharm. Bull.*, 37(4):1047–1050.
6. Hodge, I.M. (1995) Physical aging in polymer glasses. *Science*, 267:1945–1947.
7. Zhu, L. and Yu, L. (2010) Generality of forming stable organic glasses by vapor deposition. *Chem. Phys. Lett.*, 499:62–65.
8. Vincent, C., Willart, J.F., Lefort, R., Derollez, P., Danede, F., and Decamps, M. (2011) Solid-state amorphization kinetics of alpha lactose upon mechanical milling. *Carbohydr. Res.*, 346:2622–2628.
9. Bates, S., Kelly, R.C., Ivanisevic, I., Schields, P., Zografi, G., and Newman, A.W. (2007) Assessment of defects and amorphous structure produced in raffinose pentahydrate upon dehydration. *J. Pharm. Sci.*, 9(5):1418–1433.
10. Guo, Y., Byrn, S.R., and Zografi, G. (2000) Physical characteristics and chemical degradation of amorphous quinapril hydrochloride. *J. Pharm. Sci.*, 89(1):128–143.
11. Ahlneck, C. and Zografi, G. (1990) The molecular basis of moisture effects on the physical and chemical stability of drugs in the solid state. *Int. J. Pharm.*, 62:87–95.
12. Bates, S., Zografi, G., Engers, D., Morris, K., Crowley, K., and Newman, A.W. (2006) Analysis of amorphous and nanocrystalline solids from their X-ray diffraction patterns. *Pharm. Res.*, 23(10):2333–2348.
13. Dykhne, T., Taylor, R., Florence, A., and Billinge, S.J.L. (2011) Data requirements for the reliable use of atomic pair distribution functions in amorphous pharmaceutical fingerprinting. *Pharm. Res.*, 28:1041–1048.
14. Finney, J.L. (1970) Random packings and the structure of simple liquids: II. The molecular geometry of simple liquids. *Proc. R. Soc. Lond. A*, 319:495–507.
15. Silescu, H. (1999) Heterogeneity at the glass transition: a review. *J. Non-Cryst. Solids*, 243:81–108.

16. Williams, G. and Watts, D.C. (1970) Non-symmetrical dielectric relaxation behavior arising from a simple empirical decay function. *Trans. Faraday Soc.*, 66:80–85.
17. Schonhals, A., Kremer, F., Hofmann, E., Fischer, E.W., and Schlosser, E. (1993) Anomalies in the scaling of the dielectric α-relaxation. *Phys. Rev. Lett.*, 70:3459–3462.
18. Swallen, S.F. and Ediger, M.D. (2011) Self-diffusion of the amorphous pharmaceutical indomethacin near T_g. *Soft Matter*, 7:10339–10344.
19. Angell, C.A. (1988) Perspectives on the glass transition. *J. Phys. Chem. Solids*, 49(8):863–871.
20. Crowley, K. and Zografi, G. (2001) The use of thermal methods for predicting glass-former fragility. *Thermochim. Acta*, 380:79–83.
21. Plazek, D.J. and Magill, J.H. (1968) Physical properties of aromatic hydrocarbons: IV. Analysis of the temperature dependence of the viscosity and the compliance of 1,3,5,-tri-α-naphthylbenzene. *J. Chem. Phys.*, 49:3678–3883.
22. Andronis, V. and Zografi, G. (1998) The molecular mobility of supercooled indomethacin as a function of temperature and relative humidity. *Pharm. Res.*, 15(6):835–842.
23. Zhu, L., Brian, C.W., Swallen, S.F., Straus, P.T., Ediger, M.D., and Yu, L. (2011) Surface self -diffusion of an organic glass. *Phys. Rev. Lett.*, 106:256103.
24. Johari, G.P. and Goldstein, M. (1970) Viscous liquids and the glass transition: II. Secondary relaxations in glasses of rigid molecules. *J. Chem. Phys.*, 53(6):2372–2388.
25. Vogel, M., Tschirwitz, C., Schneider, G., Koplin, C., Medick, P., and Rrossler, E. (2002) A 2H NMR and dielectric spectroscopy study of the slow β-process in organic glass formers. *J. Non-Cryst. Solids*, 307–310:326–335.
26. Ngai, K. and Paluch, M. (2004) Classification of secondary relaxation in glass-formers based on dynamic properties. *J. Chem. Phys.*, 120:857–873.
27. Hatase, M., Hanaya, M., Hikima, T., and Oguni, M. (2002) Discovery of homogeneous nucleation-based crystallization in simple glass-forming liquid of toluene below the glass transition temperature. *J. Non-Cryst. Solids*, 307–310:257–263.
28. Andronis, V. and Zografi, G. (2000) Crystal nucleation and growth of indomethacin polymorphs from the amorphous state. *J. Non-Cryst. Solids*, 271:236–248.
29. Oguni, M. (1997) Intra-cluster rearrangement model for the α-process in supercooled liquids, as opposed to cooperative rearrangement of whole molecules within a cluster. *J. Non-Cryst. Solids*, 210:171–177.
30. Hancock, B.C. and Parks, M. (2000) What is the true solubility advantage for amorphous pharmaceuticals? *Pharm. Res.*, 17:397–404.
31. Murande, S.B., Pikal, M.J., Shanker, R.M., and Bogner, R.H. (2009) Solubility advantage of amorphous pharmaceuticals I. *J. Pharm. Sci.*, 99:1254–1264.
32. Ozaki, S., Minamisono, T., Yamashita, T., Kato, T., and Kushida, I. (2012) Supersaturation–nucleation behavior of poorly soluble drugs and its impact on the oral absorption of drugs in thermodynamically high-energy forms. *J. Pharm. Sci.*, 101:214–222.
33. Lu, Q. and Zografi, G. (1998) Phase behavior of binary and ternary amorphous mixtures containing indomethacin, citric acid and PVP. *Pharm. Res.*, 15:1202–1206.
34. Flory, P.J. (1953) *Principles of Polymer Chemistry*, Cornell University Press, Ithaca, NY.
35. Newman, A., Engers, D., Bates, S., Ivanisevic, I., Kelly, R.C., and Zografi, G. (2008) Characterization of amorphous API:polymer mixtures using X-ray diffraction. *J. Pharm. Sci.*, 97(11):4840–4856.

36. Cheung, M.K., Wang, J., Zheng, S., and Mi, Y. (2000) Miscibility of poly(epichlorohydrin)/poly(vinyl acetate) blends investigated with high resolution solid-state ^{13}C NMR. *Polymer*, 41:1469–1474.
37. Pham, T.N., Watson, S.A., Edwards, A.J., Chavda, M., Clawson, J.S., Stroheim, M., and Vogt, F.G. (2010) Analysis of amorphous solid dispersions using 2D solid-state NMR and ^{1}H T_1 relaxation measurements. *Mol. Pharm.*, 7:2194–2206.
38. Gordon, M. and Taylor, J.S. (1952) Ideal copolymers and the second-order transition of synthetic rubbers: I. Noncrystalline co-polymers. *J. Appl. Chem.*, 2:493–500.
39. Couchman, P.R. and Karasz, F.E. (1978) A classical thermodynamic discussion on the effect of composition on glass transition temperature. *Macromolecules*, 11:117–119.
40. Fox, T.G. (1956) Influence of diluent and copolymer composition on the glass transition temperature of a polymer system. *Bull. Am. Phys. Soc.*, 1:123.
41. Crowley, K.J. and Zografi, G. (2002) Water vapor absorption into amorphous hydrophobic drug/poly(vinylpyrrolidone) dispersions. *J. Pharm. Sci.*, 91:2150–2165.
42. Zhang, J. and Zografi, G. (2001) Water vapor absorption into amorphous sucrose-poly(vinylpyrrolidone) and trehalose-poly(vinylpyrrolidone) mixtures. *J. Pharm. Sci.*, 90:1375–1385.
43. Matsumoto, T. and Zografi, G. (1999) Physical properties of solid molecular dispersions of indomethacin with poly(vinylpyrrolidone) and poly(vinylpyrrolidone-*co*-acetate) in relation to indomethacin crystallization. *Pharm. Res.*, 16(11):1722–1728.
44. Shamblin, S.L., Taylor, L.S., and Zografi, G. (1998) Mixing behavior of colyophilized binary systems. *J. Pharm. Sci.*, 87:694–701.
45. Kougaz, K. and Clas, S.D. (2000) Crystallization inhibition in solid dispersions of MK-0591 and poly(vinylpyrrolidone) polymers. *J. Pharm. Sci.*, 89:1325–1334.
46. Newman, A.W., Knipp, G., and Zografi, G. (2012) Assessing the performance of amorphous solid dispersions. *J. Pharm. Sci.*, 101:1355–1377.
47. Tao, J., Sun, Y., Zhang, G.G.Z., and Yu, L. (2009) Solubility of small molecule crystals in polymers: D-mannitol in PVP, indomethacin in PVP/VA and nifedipine in PVP/VA. *Pharm. Res.*, 26(4):855–864.
48. Taylor, L.S. and Zografi, G. (1997) Spectroscopic characterization of interactions between PVP and indomethacin in amorphous molecular dispersions. *Pharm. Res.*, 14:1691–1698.
49. Cai, T., Zhu, L., and Yu, L. (2011) Crystallization of organic glasses: effects of polymer additives on bulk and surface crystal growth in amorphous nifedipine. *Pharm. Res.*, 28:2458–2466.
50. Newman, A.W., Reutzel-Edens, S.M., and Zografi, G. (2008) Characterization of the "hygroscopic" properties of active pharmaceutical ingredients. *J. Pharm. Sci.*, 97:1047–1059.
51. Ewing, G.E. (2005) H_2O on NaCl: from single molecule to clusters, to monolayer, to thin film, to deliquesce. *Intermolecular Forces and Clusters II*, Structure and Bonding, Vol. 116, Springer, pp. 1–25.
52. Andronis, V., Yoshioka, M., and Zografi, G. (1997) Effects of sorbed water on the crystallization of indomethacin from the amorphous state. *J. Pharm. Sci.*, 86:346–351.
53. Friesen, D.T., Shanker, R., Crew, M., Smithey, D.T., Curatolo, W.J., and Nightingale, J.A.S. (2008) Hydroxypropylmethylcellulose acetate succinate-based spray-dried dispersions: an overview. *Mol. Pharm.*, 5:1003–1019.
54. Alonso, D.E., Zhang, G.G.Z., Zhou, D., Gao, Y., and Taylor, L.S. (2009) Understanding the behavior of amorphous pharmaceutical systems during dissolution. *Pharm. Res.*, 27:608–618.

55. Hevbare, G.A., Liu, H., Edgar, K.J., and Taylor, L.S. (2013) Maintaining supersaturation in aqueous drug solutions: impact of different polymers on induction times. *Cryst. Growth Des.*, 13:740–751.
56. Hevbare, G.A. and Taylor, L.S. (2013) Liquid–liquid phase separation in highly supersaturated aqueous solutions of poorly water-soluble drugs: implications for solubility enhancing formulations. *Cryst. Growth Des.*, 13:1497–1509.